

A NEW ANATOMICALLY-PRESERVED PLANT FROM THE LOWER DEVONIAN OF
QUEBEC (CANADA): IMPLICATIONS FOR EUPHYLLOPHYTE PHYLOGENY AND
EARLY EVOLUTION OF STRUCTURAL COMPLEXITY

By

Selin Toledo

A Thesis Presented to

The Faculty of Humboldt State University

In Partial Fulfillment of the Requirements for the Degree

Master of Science in Biology

Committee Membership

Dr. Alexandru M. F. Tomescu, Committee Chair

Dr. Paul Kenrick, Committee Member

Dr. Michael Mesler, Committee Member

Dr. Gar Rothwell, Committee Member

Dr. Erik Jules, Program Graduate Coordinator

May 2018

ABSTRACT

A NEW ANATOMICALLY-PRESERVED PLANT FROM THE LOWER DEVONIAN OF QUEBEC (CANADA): IMPLICATIONS FOR EUPHYLLOPHYTE PHYLOGENY AND EARLY EVOLUTION OF STRUCTURAL COMPLEXITY

Selin Toledo

An abrupt transition in the fossil record between Early Devonian plants with simple structure and structurally-complex later Devonian plants, has frustrated efforts to understand patterns of phylogeny across the Early/Middle Devonian boundary and the evolution of complex forms. Both these aspects have important implications for lignophyte and seed plant evolution. In the first chapter, I evaluate phylogenetic relationships between the earliest seed plants, Aneurophytales, and Stenokoleales, using comprehensive taxon sampling (28 species, including all relevant permineralized species) and a set of 40 discrete and nine continuous morpho-anatomical characters. Analysis of this dataset supports the three traditional taxonomic groups (seed plants, Aneurophytales, and Stenokoleales) and place Stenokoleales among the lignophytes. In the second chapter, I characterize a new fossil plant from the Lower Devonian of Gaspé (Canada), *Kenricrana bivena* gen. et sp. nov., and I integrate it in the phylogenetic matrix developed in the first chapter. *Kenricrana* shares features with the progymnosperms, Stenokoleales, and early seed plants. Inclusion of *Kenricrana* introduces stability in the phylogenetic relationships

among these groups. *Kenricrana* is recovered as sister to the rest of the ingroup and Stenokoleales as paraphyletic to a lignophyte clade wherein aneurophytes and seed plants fall into sister clades. These results shed light on early euphyllophyte relationships and evolution, indicating early exploration of structural complexity by multiple euphyllophyte lineages and raising the possibility of a single origin of secondary growth in euphyllophytes.

ACKNOWLEDGEMENTS

I thank Francis M. Hueber, who collected the specimens containing *Aurolignia* axes. I am indebted to William DiMichele, Carol Hotton, and Jonathan Wingerath (National Museum of Natural History – Smithsonian Institution) for facilitating specimen loans; Kelly K.S. Matsunaga (University of Michigan) for help during work in the NMNH collections; Marty Reed and Casey R. Lu (Humboldt State University – HSU) for assistance with scanning electron microscopy; David S. Baston (CNRS Core Facility, HSU) for maintaining and allowing access to microscopic imaging equipment and computing capabilities; Ignacio H. Escapa and Andres Elgorriaga (CONICET & Museo Paleontologico Egidio Feruglio) for phylogenetics advice and for rendering the time-calibrated phylogeny, respectively Alexander C. Bippus for his advice on phylogenetics and computing the analyses; and Ian Cullimore, Nikole Ilse, and Laura Lea Davis for assistance in processing fossil material. I gratefully acknowledge funding for this research from the Geological Society of America Research Awards, the Paleontological Society Stephen J. Gould Student Research Award, a HSU Masters Student Research Award.

TABLE OF CONTENTS

ABSTRACT.....	2
ACKNOWLEDGEMENTS.....	4
1. CHAPTER 1: Buried deep beyond the veil of extinction: euphyllophyte relationships at the base of the spermatophyte clade	7
1.1. Introduction.....	7
1.2. Materials and methods.....	9
1.2.1. Taxon selection	9
1.2.2. Character definition and scoring.....	11
1.2.3. Phylogenetic analyses	14
1.3. Results.....	14
1.3.1. Analysis 1 (discrete characters only)	15
1.3.2. Analysis 2 (discrete + continuous characters)	15
1.3.3. Clades and synapomorphies.....	16
1.4. Discussion.....	18
1.4.1. Current understanding of relationships.....	18
1.4.2. Phylogeny and classical taxonomy	20
1.4.3. Outlier taxa.....	23
1.4.4. Broader phylogenetic patterns	27
1.5. Conclusions and future outlook	32
Literature cited.....	36
Figures	42
Appendix A.....	44
Appendix B.....	47

Appendix C	54
Appendix D.....	58
Appendix E	60
Appendix F	61
2. CHAPTER 2: An Emsian radiatopsid updates early euphyllophyte phylogeny pointing to Early Devonian exploration of structural complexity by multiple basal lineages	63
2.1. Introduction.....	63
2.2. Materials and Methods.....	65
2.2.1. Fossil material	65
2.2.2. Phylogenetic analyses	66
2.3. Results.....	67
2.3.1. Systematics	67
2.3.2. Phylogenetic position of Kenricrana.....	77
2.4. Discussion	79
2.4.1. Phylogenetic relationships	79
2.4.2. Evolution of plant structure	82
2.5. Conclusions.....	84
References.....	86
Supporting Information.....	91
Figures	92

1. CHAPTER 1: BURIED DEEP BEYOND THE VEIL OF EXTINCTION:
EUPHYLLOPHYTE RELATIONSHIPS AT THE BASE OF THE SPERMATOPHYTE
CLADE

1.1. Introduction

The Devonian period (ca 358-400 Ma) witnessed key events and processes for the evolutionary history of vascular plants (Bateman et al., 1998). The evolutionary radiation that gave rise to all euphyllophyte lineages started in the Early Devonian and by the Middle and Late Devonian most of the major groups with living representatives were present. A major aspect of this evolutionary history is the origin of seed plants (spermatophytes), which is still poorly understood. Because seed plants arose early in the history of plant life (no later than the Givetian, ca. 385 Ma ago; Prestianni and Gerrienne, 2010) and their closest hypothesized relatives among seed-free plants are all extinct Devonian plants, the key to the origin and early evolution of seed plants lies in the fossil record.

Traditionally, discussions of seed plant evolution have included two extinct groups, the progymnosperms and Stenokoleales. Progymnosperms are free-sporing euphyllophytes with gymnosperm-like (pycnoxylic) wood (Beck, 1960a). Among progymnosperms, the aneurophytes are characterized by actinosteles (ribbed protosteles), like the earliest seed plants, whereas the archaeopterids typically have eusteles (Beck, 1976). Aneurophytes are known as early as the Eifelian (ca. 390 Ma) and are also

characterized by tridimensional branching systems bearing ultimate appendages with terete primary xylem (Beck, 1976). The archaeopterids are known starting in the Givetian (ca. 385 Ma) and exhibit typically extensive secondary growth (Beck, 1976). The Stenokoleales, also known as early as the Eifelian, are characterized by actinosteles with protoxylem parenchyma and by axes bearing appendages bifurcated at the base, which is typically pulvinus-like (Beck and Stein, 1993).

Both Stenokoleales and progymnosperms have been proposed as potential precursors of the seed plants (Matten and Banks, 1969; Bonamo, 1975; Beck, 1976; Rothwell and Erwin, 1987; Matten, 1992, 1996; Beck and Stein, 1993). Previous phylogenetic studies have looked at the relationships between these groups and seed plants (Matten, 1992; Galtier and Meyer-Berthaud, 1996; Kenrick and Crane, 1997; Rothwell and Serbet, 1994; Hilton and Bateman, 2006; Momont, 2015). However, part of those studies addressed relationships of narrower groups (e.g., relationships primarily among seed plants; Rothwell and Serbet, 1994; Hilton and Bateman, 2006) or of much broader groups (e.g., tracheophytes, embryophytes; Kenrick and Crane, 1997). Additionally, these studies of broader or narrower focus did not include Stenokoleales. The few studies focused more specifically on relationships between early seed plants, progymnosperms, and Stenokoleales, employed low numbers of taxa (e.g., only one representative for each major group) or characters (between nine and 29 characters).

Among progymnosperms, aneurophytes are considered more likely to include a seed plant ancestor than the archaeopterids, because the earliest seed plants (e.g. *Elkinsia* Rothwell, Scheckler et Gillespie) possess actinosteles and not eusteles, like the

archaeopterids or younger seed plants (Rothwell and Erwin, 1987). The Stenokoleales also share the actinostelic condition. Here we evaluate phylogenetic relationships between these early euphyllophytes characterized by actinostelic xylem architecture and traditionally associated with the origin of seed plants, and the early, actinostelic seed plants. This study includes the most comprehensive taxon sampling relevant to this question, to date, and considers all anatomically preserved species that belong to the three major groups, as well as several species of unresolved taxonomic placement. The study employs anatomical and morphological characters, including continuous characters, which quantify continuously varying features such as sizes and size ratios. Our phylogenetic analyses recover monophyletic seed plants, Stenokoleales, and aneurophytalan progymnosperms, with the latter placed as sister to a clade including the former two (and termed the bilateral clade). Traditional taxonomic groups are, thus, supported in this phylogeny and Stenokoleales are recovered in a position nested among the lignophytes. We find that continuous characters bear a phylogenetic signal and improve resolution considerably. Our results suggest a Givetian minimum age for the seed plant ancestor, a late Emsian minimum age for the Stenokoleales, and early Emsian minimum ages for the bilateral clade, the aneurophyte ancestor, and the lignophytes.

1.2. Materials and methods

1.2.1. Taxon selection—

This study includes 28 anatomically-preserved taxa known from permineralized specimens (Appendix 1). Nine of these are early seed plants or putative seed plants:

Calathopteris heterophylla Long, *Elkinsia polymorpha* Rothwell, Scheckler et Gillespie, *Laceyia hibernica* May et Matten, *Tetrastichia bupatides* Gordon, *Triradioxylon primaevum* Barnard et Long, *Tristichia longii* Galtier, *Tristichia ovensi* Long, *Tristichia tripes* Galtier et Meyer-Berthaud, and *Yiduxylon trilobum* Wang et Liu; six are placed in the Stenokoleales: *Brabantophyton runcariense* Momont, Gerrienne et Prestianni, *Crossia virginiana* Beck et Stein, *Stenokoleos bifidus* Matten et Banks, *Stenokoleos holmesii* Matten, *Stenokoleos setchelli* Hoskins et Cross, and *Stenokoleos simplex* Beck; eight have been classified as aneurophytalean progymnosperms: *Aneurophyton germanicum* Kräusel et Weyland, *Proteokalon petryi* Scheckler et Banks, *Reimannia aldenense* Arnold, *Rellimia thomsonii* Leclercq et Bonamo, *Tetraxylopteris schmidtii* Beck, *Triloboxylon ashlandicum* Scheckler et Banks, and *Triloboxylon arnoldii* Matten. Aside from these groups, we included *Actinoxylon banksii* Matten, a species described initially as a pityalean progymnosperm (Matten, 1968) and discussed by Beck (1976) as a potential archaeopteridalean progymnosperm. We also included three euphyllophytes of unresolved taxonomic affinities: the Emsian plant described by Gensel (1984) from the Battery Point Formation of Gaspé (Canada), *Gothanophyton zimmermanni* Remy et Hass (Emsian), and *Langoxylon asterochlaenoideum* Scheckler, Skog et Banks (Givetian). The outgroup used to root the analyses is *Psilophyton dawsonii* Banks, Leclercq et Hueber. This plant is the best characterized early euphyllophyte, to date, in terms of anatomy and morphology, and predates younger and structurally more complex Devonian euphyllophytes (Banks et al., 1975).

1.2.2. Character definition and scoring—

We used a total of 49 characters, of which 40 are discrete characters (33 anatomical, seven morphological) and nine are continuous characters (five of them are ratios and four are absolute sizes) (Appendix 2). The matrix was assembled in Mesquite 3.2 (Maddison and Maddison, 2009). Characters were scored from the literature. Overall, the matrix has 10.23% missing data: 11.34% for the discrete characters and 5.56% for continuous characters (Appendix 3, 4).

Continuous characters have been shown to add phylogenetically useful information that may not be codified in discrete character states (Escapa and Pol, 2011). Here, continuous characters (Appendix 3) are each based on a single measurement. In order to avoid over-emphasizing small differences between taxa, these measurements were converted into ranges by adding and subtracting 10% from the measured value. The ranges were subsequently standardized to be equivalent to one step of a discrete character by dividing the end values of each range (maximum and minimum) by the highest overall maximum of the character across the entire set of taxa. This was done to avoid variation in character weighting resulting from the magnitude of absolute values.

Only one of the discrete anatomical-morphological characters (Appendix 4) is not vegetative, because reproductive structures are known in very few of the taxa included in this study: *Psilophyton*, *Rellimia*, *Tetraxylopteris*, *Aneurophyton*, and *Elkinsia* (Banks, 1957; Matten and Banks, 1967; Banks et al., 1975; Scheckler, 1976; Bonamo, 1977; Serlin and Banks, 1978; Schweitzer and Matten, 1982; Rothwell et al., 1989; Serbet and Rothwell, 1992; Dannenhoffer et al., 2007).

In coding the morphology of the Devonian plants into discrete characters, we strived to avoid introducing *a priori* homology assumptions and to consider how morphology and anatomy may have related to development in these plants (based on current knowledge of development in living plant lineages). As a result, some characters introduce novel perspectives on basic determinants of sporophyte organization. One of these is a character (10) implying that sporophyte axes fall into two major types with distinctly different modes of development that lead to an internal organization exhibiting either radial symmetry (termed the radial organographic domain) or bilateral symmetry (bilateral organographic domain). These two modes of development are underpinned by different regulatory programs and, in plants that possess both types, the development of axes with bilateral symmetry on radially symmetrical subtending axes marks a switch from one regulatory program to the other, in a way similar to the onset of specific leaf developmental programs at the shoot apical meristem in derived euphyllophytes (Sanders et al., 2007; Lenhard, 2017).

In another example, the presence of adaxial-abaxial polarity (character 44), whose determinants are not known in these extinct plants, was inferred based on presence of asymmetry between the adaxial and abaxial sides of primary xylem in the traces of laterals. Features such as adaxial concavity of the trace, asymmetry in the position of protoxylem strands within the trace, or asymmetry in the outline of the trace (e.g. abaxially but not adaxially lobed) were interpreted as marks of adaxial-abaxial polarization of tissue development.

Characters based on histology of the cortex are also relevant to how the sporophyte of these Devonian plants developed. For instance, presence of more than one cell type in the cortex (e.g. parenchyma and sclerenchyma) indicates differential gene expression in different regions of the cortex. Thus, differentiation of cortical regions that are consistently distinct in cell type must be a result of partitioning of the cortex volume into developmental domains specified by distinct regulatory programs, such as partitioning into concentric layers (e.g., bands of sclerenchyma nests in the inner cortex) or into radial sectors (e.g., alternating parenchymatous and sclerenchymatous areas around the periphery of axes, in the outer cortex, as seen in *Dictyoxylon*-type organization).

Similarly, protoxylem architecture (characters 17-19) must reflect patterns of polar auxin transport in the developing tip of axes. In living seed plants, basipetal auxin flow from leaf primordia causes development of the sympodia that characterize their eusteles (Benková et al. 2003). These correspond to protoxylem strands that do not converge into a central strand, which is also absent in the Devonian euphyllophytes with permanent protoxylem architecture (*sensu* Beck and Stein, 1993), such as cladoxyloids, as well as in some early seed plants (e.g., *Tristichia longii*). Currently, we do not know what patterns of polar auxin transport were like at the tips of Devonian plant axes. However, if polar auxin flow from the apical meristem was involved in procambial development of the Devonian euphyllophyte axes, a radiate protoxylem architecture (i.e., characterized by convergence of protoxylem strands from lateral into a central

protoxylem strand of the main axis) would have necessitated convergence of auxin transport pathways from laterals into a single central stream.

1.2.3. Phylogenetic analyses—

Phylogenetic searches were conducted in TNT 1.5 (Goloboff and Catalano, 2016), using equally-weighted parsimony as the optimality criterion. 50,000 trees were held in the memory using the command “hold 50,000”. The parsimony analyses were initiated using the command “xmult=hits10”. Using this command, the analysis departs from 50 random addition sequences (RAS), followed by tree bisection-reconnection. The resulting trees were submitted to a combination of Ratchet (default options), Tree Drifting (default options), and sectorial searches (default options). Bootstrap values were generated using the “bootstrap resampling” command with standard tree search parameters and 100 replicates. CI and RI were calculated using the “stats.run” script provided with the TNT installation package.

We used two character sampling regimes in two different analyses. The first tree search (Analysis 1) was run using only discrete characters. The second analysis included discrete plus continuous characters (Analysis 2). All characters were equally weighted and unordered to avoid introducing bias from *a priori* assumptions. The time calibrated tree was produced with R software (R Core Team, 2017) utilizing the ‘timePaleoPhy’ and ‘geoscalePhylo’ functions of the *paleotree* and *strap* packages, respectively (Bapst, 2012; Bell and Lloyd, 2015).

1.3. Results

1.3.1. Analysis 1 (discrete characters only)—

This search resulted in 19 most parsimonious (MP) trees (tree length 84; CI = 0.548, RI = 0.683). In the strict consensus tree (Appendix 5), the ingroup forms a large polytomy that includes only two resolved clades. One of these consists of two aneurophytes (*Tetraxylopteris* and *Proteokalon*), whereas the other includes the seed plants (except for *Yiduxylon*), with *Tristichia tripos* sister to the remaining seed plants, which form a polytomy.

1.3.2. Analysis 2 (discrete + continuous characters)—

Addition of continuous characters led to full resolution: we recovered a single MP tree (tree length 96.4330; CI = 0.528, RI = 0.656) (Fig. 1 and Appendix 6). The putative aneurophyte *Reimannia* is recovered as sister to the rest of ingroup species. An aneurophyte clade (Fig. 1) consists of *Aneurophyton* and *Cairoa* forming a grade basal to the divergence of two clades, one including *Triloboxylon ashlandicum* and *Rellimia*, while the other includes *Proteokalon* and *Tetraxylopteris*. The aneurophyte clade is sister to a larger clade, characterized by the presence of an organographic domain that exhibits bilateral symmetry and termed the “bilateral clade” (Fig. 1), in which *Yiduxylon* (putative seed plant) and *Actinoxylon* (putative progymnosperm) form a basal grade. A major dichotomy separates this larger clade into two clades, one including seed plants, while the other includes the Stenokoleales. In the former, *Triloboxylon arnoldii* is sister to the seed plant clade (Fig. 1); in the latter, Gensel’s (1984) plant and *Langoxylon* form a grade basal to the Stenokoleales (Fig. 1). Within the seed plant clade, *Tristichia tripos* is sister to the remaining seed plants, which are resolved in two clades: one in which *Tetrastichia*

is sister to *Calathopteris* + *Elkinsia*, and one in which *Triradioxylon* + *Tristichia ovensi* is sister to *Laceyia* + *Tristichia longii*. Within the Stenokoleales, *Brabantophyton* + *Crossia* is sister to a clade consisting of grade that includes *Gothanophyton* and *Stenokoleos simplex* basal to *S. holmesii* + *S. bifidus*.

1.3.3. Clades and synapomorphies—

The results of Analysis 2 provide synapomorphies that support each clade. The seed plant clade (exclusive of *Yiduxylon*) (Fig. 1) is supported by the presence of pulvinus-like branch bases (character 36). This character is also the synapomorphy that defines the *Stenokoleos* clade, and is present in *Crossia*, which implies that pulvinus-like branch bases evolved independently in these groups. It is worth noting that *Tristichia*, a genus classified among the seed plants, is polyphyletic, with one species (*T. tripos*) sister to all other seed plants, whereas the other two (*T. ovensi* and *T. longii*) are each part of a different clade within the seed plants.

The synapomorphies that unite the Stenokoleales in a monophyletic group (including a *Stenokoleos* clade, as well as a *Brabantophyton* + *Crossia* clade, sister to the clade formed by *Gothanophyton* and *Stenokoleos*; Fig. 1) are the traces supplying the bilateral organographic domain, which consist of more than one vascular bundle (character 42), with the bundles diverging tangentially from the tip of a xylem rib (character 35), and the bipartite architecture of the bilateral organographic domain (at its base, which is the only known portion of it) (character 45). Some of these features are present also in *Yiduxylon*, *Triloboxylon arnoldii*, and *Tristichia longii*, suggesting that traces to the bilateral domain consisting of multiple vascular bundles with tangential

divergence may have evolved independently in other groups. The stenokolealean clade is also characterized by the highest values of the ratio of maximum primary xylem diameter to maximum axis diameter (character 0); similar values (> 0.6) are found outside of this clade only in Gensel's (1984) plant.

The larger clade formed by the two sister clades each of which includes the seed plant clade (with *Triloboxylon arnoldii* as sister group) and the stenokolealean clade [with the Gensel (1984) plant - *Langoxylon* grade at the base], respectively (Fig. 1), is united by the architecture of the vascular supply to the bilateral domain, wherein traces that diverge from the primary xylem ribs do not exhibit further divergence as they enter the base of appendages with bilateral symmetry (character 43).

The aneurophyte clade (exclusive of *Triloboxylon arnoldii* and *Reimannia*; Fig. 1) is supported by the presence of recurring appendages with terete xylem (character 37) and also by two continuous characters: an increase in the ratio of primary xylem to axis surface area (as seen in cross section) (character 1) and lowest metaxylem tracheid diameter values (in the radial organographic domain; character 4).

We recovered a large lignophyte clade (Fig. 1), which includes all ingroup taxa, except for *Reimannia* (a putative aneurophyte in which secondary growth, if present, has yet to be discovered). The clade is supported by the presence of secondary xylem (character 26). However, in the current tree topology, this character shows a reversal to absence of secondary growth in the ancestor of the clade including Gensel's (1984) plant + *Langoxylon* + Stenokoleales, and a further reversal to presence in the *Brabantophyton* + *Crossia* clade, within the Stenokoleales.

1.4. Discussion

1.4.1. Current understanding of relationships—

A small number of studies have addressed questions of phylogeny with implications for the relationships of Devonian euphyllophytes traditionally associated with the origin of seed plants. Rothwell and Serbet (1994) and Hilton and Bateman (2006) were concerned primarily with the relationships among major seed plant lineages and included progymnosperms as outgroups. The focus of Matten (1992) and Galtier and Meyer-Berthaud (1996) was on the relationships among the earliest seed plant groups and they also addressed relationships between seed plants, Stenokoleales, and progymnosperms. In the most recent analysis, Momont (2015) addressed relationships between major euphyllophyte groups, including progymnosperms, Stenokoleales, and seed plants.

Rothwell and Serbet (1994) and Hilton and Bateman (2006) did not include Stenokoleales in their analyses. Both these studies sampled extensively seed plant diversity including all living and extinct gymnosperm groups, as well as angiosperms, but included only three progymnosperms representing the aneurophytes, archaeopterids, and cecropsids. Both the study by Matten (1992) and the one by Galtier and Meyer-Berthaud (1996) included Stenokoleales and progymnosperms. Whereas Galtier and Meyer-Berthaud (1996) sampled six protostelic early seed plants, Matten (1992) included only two terminals for seed plants, each representing a composite concept of a ‘Lyginopteridales plant’ and a ‘Calamopityales plant’ based on seven and four genera, respectively. In both studies, the Stenokoleales and the progymnosperms (only

aneurophytes in Galtier and Meyer-Berthaud's study; aneurophytes and archaeopterids in Matten's study) are also included as single terminals represented by composite plant concepts drawn from several species or genera. Momont's (2015) analysis included four aneurophytes (*Rellimia*, *Aneurophyton*, *Triloboxylon ashlandicum*, and *Tetraxylopteris*), one archaeopterid (*Callixylon*), three Stenokoleales (*Stenokoleos holmesii*, *S. simplex*, and *Brabantophyton*), and two seed plants (*Elkinsia* and *Tristichia tripos*). Aside from these, the analysis also included basal euphyllophytes (*Psilophyton* and *Armoricaphyton*) and cladoxylopsids (one pseudosporochnalean and one iridopterid).

In Hilton and Bateman's (2006) analysis, rooted with the aneurophyte *Tetraxylopteris*, progymnosperms (*Tetraxylopteris* and an *Archaeopteris* + *Cecropsis* group) and seed plants form a basal polytomy. Rothwell and Serbet (1994) used a theoretical set of ancestral characters states to root their analysis and recovered an archaeopterids + cecropsids group sister to the seed plants, in a clade that is sister to the aneurophytes. These relationships were recovered consistently and only collapsed in a polytomy when parsimony was relaxed to MP + 2 steps. Matten (1992) also recovered a polytomy between aneurophytes, archaeopterids, and seed plants, when Stenokoleales were excluded from analyses. When included, Stenokoleales resolved as sister to seed plants in a clade that was sister to a progymnosperm clade (aneurophytes + archaeopterids). In Galtier and Meyer-Berthaud's (1996) study, Stenokoleales are sister to seed plants. However, this may be a result of using only aneurophytes and Stenokoleales as outgroups, each as a single terminal (composite plant concept), with the analysis rooted by the aneurophyte lineage. Finally, in Momont's (2015) phylogenetic

analysis rooted with *P. dawsonii*, the Stenokoleales and seed plants form a large polytomy, with the archaeopterid as the sister group. Basal to this clade, Aneurophytales form a paraphyletic group. The cladoxylopsids form a clade that is sister to the progymnosperm + Stenokoleales + seed plants clade.

Among these studies, three included Stenokoleales in addition to Aneurophytales and seed plants (Matten, 1992; Galtier and Meyer-Berthaud, 1996; Momont, 2015). In all these studies, Stenokoleales and the seed plants form a clade. However, (1) in Galtier and Meyer-Berthaud's study, this relationship is constrained by the choice and number of taxa – see above; and (2) in Matten's and Momont's analyses, relationships within the Stenokoleales + seed plants clade are unresolved [polytomy in Momont (2015) and each of the two groups represented by a single terminal in Matten (1992)]. Whereas in Matten's study the progymnosperms (aneurophytes + archaeopterids) form a clade that is sister to Stenokoleales + seed plants, in Momont's analysis, the progymnosperms form a paraphyletic grade basal to Stenokoleales + seed plants.

1.4.2. Phylogeny and classical taxonomy—

Our analysis (Analysis 2) recovers an aneurophyte clade (exclusive of *Reimannia aldenense* and *Triloboxylon arnoldii*, both classified at least tentatively as aneurophytes – see below), a Stenokoleales clade (including *Gothanophyton zimmermanni*, a plant of unresolved affinities), and a seed plant clade (exclusive of *Yiduxylon trilobum*, which was discussed as a putative seed plant; Wang and Liu, 2015). Recovery of an aneurophyte clade is in contrast to the results of the only previous analysis that included more than one aneurophyte progymnosperm (Momont, 2015), which recovered aneurophytes as a

paraphyletic group. However, if *Reimannia* is an aneurophyte, our results also support the paraphyletic status of aneurophytalan progymnosperms, and if *Triloboxylon arnoldii* is an aneurophyte, the implication is that aneurophytes are polyphyletic.

In previous analyses, the seed plant clade was placed as sister to a clade including the Stenokoleales. Broadly consistent with this hypothesis of relationships, we recover seed plants and Stenokoleales in two sister clades in which each of them is accompanied by “outlier” species: *Triloboxylon arnoldii*, a putative aneurophyte, forms a clade with the seed plants; *Langoxylon asterochlaenoideum* and Gensel’s (1984) plant form a grade at the base of the Stenokoleales.

The clades representing the three major taxonomic groups are supported by minimal numbers of discrete synapomorphies – one each for the aneurophyte and seed plant clades, and three for the Stenokoleales – and bootstrap support values are low (Appendix 6). This situation is likely due to the constraints of our data set, including the relatively simple morphology of the plants, which limits the number of characters that can be defined; a general lack of knowledge of reproductive structures (with very few exceptions: *Psilophyton*, *Rellimia*, *Tetraxylopteris*, *Aneurophyton*, and *Elkinsia*), which further limited the number of characters; the fragmentary nature of the species included, which resulted in uneven numbers of characters that could be scored across species; the broad taxonomic sampling, which, due to the fragmentary nature of species, further limited the number of characters that could be scored across most taxa in the dataset and, therefore, used in the analysis; and relatively high levels of homoplasy of anatomical characters. The lack of resolution in the results of Analysis 1 (discrete characters only)

is, thus, not very surprising. Nevertheless, the majority rule consensus tree resulting from the analysis based exclusively on discrete characters (Appendix 7) shows that the same seed plant clade and aneurophyte clade recovered by the analysis including both discrete and continuous characters, as well as a *Stenokoleos* clade, are recovered in at least 68% of MP trees (68% for the aneurophyte clade, 73% for the *Stenokoleos* clade, and 100% for the seed plant clade). However, the same majority rule consensus tree also suggests that *Brabantophyton*, *Crossia*, and *Gothanophyton* are not recovered as part of a clade with *Stenokoleos* in a high number of MP trees, and shows that aneurophytes (and not *Stenokoleales*) are recovered as more closely related to seed plants in only slightly more than half of the MP trees (52%).

The outlier species in our results reflect problems in the taxonomy of Devonian euphyllophytes characterized by lobed protosteles. These are mostly due to discrepancies between theoretical concepts of higher taxa (e.g., progymnosperms, Aneurophytales, seed plants) and the realities of diagnostic characters preserved in specimens. For instance, not all species classified as progymnosperms (therefore, lignophytes) have been demonstrated to possess secondary growth, let alone from a bifacial cambium; additionally, reproductive structures are not known for all the species placed among progymnosperms (Bonamo, 1975; Beck, 1976). Likewise, most of the earliest species classified as seed plants preserve no evidence of reproductive structures to ascertain their seed plant identity (e.g. Galtier and Meyer-Berthaud, 1996; Dunn and Rothwell, 1992; Wang and Liu, 2015). Furthermore, for the *Stenokoleales*, little is known about the architecture and anatomy of their branching systems and no reproductive structures have

been documented (Beck, 1960b; Matten and Banks, 1969; Matten, 1992; Momont et al., 2016b). Another major issue is that different species are known at different levels of anatomical and morphological detail, making for uneven coverage in terms of comparisons and character scoring. As a result of all these, previous taxonomic assignments of several of the species considered here have been based on comparisons and characters other than those that are diagnostic for the respective higher taxa. This could explain at least in part why our phylogeny (Analysis 2) does not fully match the traditional taxonomic placements of some of the species (outlier taxa).

1.4.3. Outlier taxa—

In the case of *Triloboxylon arnoldii*, considered an aneurophytalan progymnosperm, Stein and Beck (1983) have pointed out that (1) emission of traces to laterals that consist of paired vascular bundles, along with (2) the presence of sclerenchyma in the inner cortex, set this species apart from the concept of a typical aneurophyte. Indeed, in our analysis *T. arnoldii* is recovered nested well within the bilateral clade, as sister to a seed plant clade, with which it shares numerous features; the clade formed by seed plants + *Triloboxylon arnoldii* has presence of scattered sclerenchyma in the inner cortex (character 29) as a synapomorphy. Its sister group relationship with the seed plant clade raises the possibility that the species reconstructed as *T. arnoldii* may represent seed plant remains. However, as pointed out by Stein and Beck (1983), the significant size difference between the main axes of *T. arnoldii* and the much smaller size of the traces to lateral appendages documented on these axes suggests alternative interpretations. It is possible that these traces supplied fertile appendages, as suggested by their resemblance

to the anatomy of reproductive organs described in aneurophytes. In turn, this suggests we may still be missing some of the vegetative parts of this plant, i.e., that *T. arnoldii* may have also had larger vegetative branching systems of intermediate size between the main axes and the putative fertile appendages (Stein and Beck, 1983), in which case those branching systems could have possessed a vascular supply of radial symmetry.

The position of *Reimannia aldenense* outside of the aneurophyte clade and as sister to all other ingroup species, is supported by several synapomorphies: regular branch taxis (character 12), lobed primary xylem (i.e. actinostele) (character 14), and metaxylem tracheids with bordered pits (character 24). The placement of *Reimannia* implies that either it is not an aneurophyte or, if it is, then aneurophytes may be a bigger group that includes additional, yet to be discovered, diversity and forms a grade at the base of the bilateral clade. While *Reimannia aldenense* has been assigned to the aneurophytes (Matten, 1973; Stein, 1982), the species shows significant anatomical differences from the typical aneurophyte, which could explain its outlying position. These include the absence of alternating bands of sclerenchyma and parenchyma in the outer cortex, tangentially produced traces (Stein, 1982) and the absence of secondary xylem (even though the possibility that *Reimannia* did produce secondary tissues cannot be ruled out, for the time being, the lack of secondary growth represents a difference from Aneurophytales). The fragmentary nature of some members of Aneurophytales (including *Reimannia* itself) as currently characterized, as well as the broad anatomical diversity present in the group (Stein, 1982), may also have contributed to the placement of *Reimannia* recovered here.

Another outlier, *Actinoxylon banksii*, was first described by Matten (1968) as a protostelic progymnosperm and was placed in the order Pityales. Subsequently, Beck (1976) dissolved the order Pityales and placed *Actinoxylon* among archaeopteridalean progymnosperms, implying a eustelic, rather than protostelic architecture. We question this assignment on two grounds: (1) Beck himself was unsure of the exact nature of tissues at the center of *Actinoxylon* axes, which he indicated with a question mark (Beck, 1976, fig. 2); (2) in the original description, Matten (1968; fig. 1, 2, 4, 5) mentions and shows tracheids in the incompletely preserved region at the center of the stele. Consequently, here we treat *Actinoxylon* as having a mesarch protostele. In the MP tree of Analysis 2, *Actinoxylon* is recovered as sister to the clade including Stenokoleales and seed plants, supported by the presence of protoxylem strands along the primary xylem ribs of the stele (character 18) as synapomorphy. One continuous character, the ratio of maximum primary xylem diameter to maximum axis diameter (character 0), also supports the clade formed by *Actinoxylon* and its sister group, reaching higher values at the base of this clade and throughout most of it. The position of *Actinoxylon* suggests that it is more closely related to seed plants than the aneurophytalean progymnosperms.

Yiduxylon trilobum, an early Devonian euphyllophyte, was putatively assigned to the seed plants by Wang and Liu (2015). These authors interpreted *Yiduxylon* as a transitional form between aneurophytes and early seed plants based on (1) presence of protoxylem strands only at the tip of the primary xylem ribs (and not along rib midplanes); (2) size of tracheids and rays in the secondary xylem, though to represent an intermediate between pycnoxylic wood (as typically attributed to aneurophytes) and

manoxylic wood (typically attributed to early seed plants); (3) presence of bordered pits on both tangential and radial walls of secondary xylem tracheids, as seen in aneurophytes but not in seed plants, which have pits only on the radial walls; (4) tangential divergence of traces to laterals (seen in seed plants; e.g., *Tristichia longii*), instead of radial divergence (as in aneurophytes). In contrast to early seed plants, in *Yiduxylon* the traces to laterals that diverge as paired vascular bundles divide further, to form four bundles per trace. Additionally, *Yiduxylon* is distinguished from the seed plants in our analysis by the absence of sclerenchyma in the inner cortex. This combination of characters is responsible for the position of *Yiduxylon* as sister to the clade formed by the other species possessing a bilateral domain.

The placement of *Yiduxylon trilobum* in our analysis indicates that this species may not be a seed plant as proposed by Wang and Liu (2015), but is consistent with those authors' interpretation of the species as an intermediate between aneurophytes and seed plants. However, current knowledge of *Yiduxylon* is relatively limited, with anatomical features such as the presence of a central protoxylem strand and metaxylem tracheid pitting type (let alone reproductive structures) still undocumented, therefore further in-depth characterization of this plant may lead to changes in its phylogenetic placement.

Gothanophyton zimmermanni is another plant of uncertain taxonomic placement that combines stenokolealean features (tangential divergence of paired bundles forming the trace to a lateral appendage) with P-type tracheid pitting, plesiomorphic among euphyllophytes. Compared by Remy and Hass (1986) with the aneurophytes, *Gothanophyton* was discussed as a putative iridopteridalean cladoxylipsoid by Scheckler

et al. (2006). In our analysis, *Gothanophyton* is nested among the Stenokoleales and sister to the *Stenokoleos* clade, with which it is united by the number of primary xylem ribs: four (or more) (character 15).

Langoxylon asterochlaenoideum, a Middle Devonian euphyllophyte, was not assigned to any specific taxonomic group by Scheckler et al. (2006). *Langoxylon* combines features of several major Devonian taxa, including the Aneurophytales (e.g. similar length of actinostele ribs with several protoxylem strands along the midplanes), Archaeopteridales (e.g. pith-like zone at the center of the stele), Stenokoleales (e.g. protoxylem parenchyma), as well as *Gothanophyton* and the Iridopteridales (H-shaped bilaterally symmetrical traces) (Scheckler et al., 2006). Our analysis recovered *Langoxylon* as sister to the Stenokoleales (including *Gothanophyton*), with which it forms a clade defined by the presence of protoxylem parenchyma (character 21) and by higher ratios between primary xylem rib basal width and maximum xylem diameter (in cross section) (character 3). The placement of *Langoxylon* suggests that, if it is not a stenokolealean, it represents a lineage closely related to the Stenokoleales. The same inference applies to Gensel's (1984) plant, recovered as sister to the *Langoxylon* + Stenokoleales clade, in a clade supported by two continuous characters – the ratio between the primary xylem size and axis size (characters 0 and 1).

1.4.4. Broader phylogenetic patterns—

In traditional taxonomic treatments, the three major taxonomic groups considered here, the aneurophytes, Stenokoleales, and seed plants, are not as distinctly different from each other, in terms of salient anatomical features, as their evolutionary relationships would

predict. This is due to (1) the small number of characters used to define these groups (particularly in the absence of known reproductive structures); (2) the broad (and sometimes overlapping) ranges of variation of these characters within each of the major taxonomic groups, and (3) outlier taxa (discussed above) that introduce “exotic” combinations of characters in each group. As a result, the sets of features that define these groups are significantly overlapping. In fact, differences within each major group can be bigger than those between the groups. Thus, it is not surprising that our analysis including only discrete characters resulted in a large polytomy, especially since only one character on reproductive biology (scored for <20% of the species) and very few based on morphology were included (see also discussion under “Phylogeny and classical taxonomy”).

In this context, it is worth noticing that addition of continuous characters related to anatomy significantly improved phylogenetic resolution, as compared to the analysis based only on discrete characters. Importantly, the continuous characters we used seem to carry phylogenetic signal for the set of taxa analyzed here, i.e., actinostelic euphyllophytes associated with the origin of seed plants. This suggests that continuous characters based on anatomy are useful for understanding relationships between these particular Devonian species and among major groups of Devonian plants. Characters that are particularly consequential include the ratio between the primary xylem size and axis size as seen in cross sections, both in terms of diameter (character 0) and surface area (character 1), as well as a measure of the slenderness of primary xylem ribs (i.e., the ratio between basal rib width and overall xylem diameter in cross section; character 3) and the

diameter of metaxylem tracheids (character 4). The conclusion that the continuous characters used here carry phylogenetic signal is supported by the fact that (1) we recovered an aneurophyte clade, a stenokolealean clade, and a seed plant clade, despite the lack of resolution for these groups in the analyses that used exclusively discrete characters, and (2) we recovered placements of most of the species that are largely congruent with the recommendations of previous taxonomic studies. Therefore, despite the low levels of support, our results provide reasonable hypotheses of relationships between the earliest seed plants and similar protostelic Devonian euphyllophytes.

Three clades including aneurophytes, seed plants, and stenokolealeans, respectively, are recovered not only in the analysis using discrete and continuous characters, but also in a high percentage of the MP trees obtained using only discrete characters, as demonstrated by the majority rule consensus tree (with the difference that in the latter tree the stenokolealean clade consists exclusively of *Stenokoleos*). The broad support for the three clades, even based primarily on vegetative anatomical characters, suggests that they may, indeed, represent natural taxa. However, relationships between the three groups are not fully and unequivocally resolved: whereas inclusion of continuous characters lends support to a closer relationship between Stenokoleales and seed plants, discrete characters alone seem to support (albeit only marginally – 52% of MP trees; Appendix 7) a closer relationship between aneurophytes and seed plants. Together, these suggest that fuller resolution of relationships with improved levels of support will require inclusion of additional characters coding for morphology and, especially, reproductive biology.

At this stage, the topology of the MP tree obtained using both discrete and continuous characters shows that continuous characters, phylogenetically significant at the level of our dataset, tip the resolution of relationships in support of a closer relationship between Stenokoleales and seed plants, by recovering them as part of the same clade. This clade is part of a larger clade (including also *Actinoxylon* and *Yiduxylon*) that is defined by organography featuring axes characterized by bilateral symmetry (as indicated at a minimum by the symmetry of their vascular tissues) – the bilateral clade (Fig. 1). Grouping of the seed plants and Stenokoleales in the same (more inclusive) clade is in agreement with Momont’s (2015) results and indicates that seed plants may share a closer ancestor with the Stenokoleales than with aneurophytealean progymnosperms.

Although the Stenokoleales continue to be a poorly understood group of euphyllophytes, their placement in a clade that includes seed plants and is sister to aneurophytes implies that they are lignophytes (Fig. 1), a possibility discussed previously on numerous occasions (Beck and Stein, 1993; Kenrick and Crane, 1997; Scheckler et al., 2006; Momont et al., 2016a). In turn, this implies that *Stenokoleos*, a genus in which secondary growth has not been demonstrated to date, may have at least harbored developmental potential for secondary growth. This inference is consistent with evidence for secondary growth in two other stenokolealeans, *Brabantophyton* and *Crossia* (Beck and Stein, 1993; Momont et al., 2016a). The same inference applies to *Langoxylon* and Gensel’s (1984) plant, two plants nested deeply within the lignophytes, according to our results, but for which secondary growth has not been documented. As a general

observation, the current absence of evidence for secondary growth in these species that are resolved in our phylogeny as lignophytes cannot be taken, on principle, as evidence for absence; and even less so if we consider that at least some regulatory mechanisms for secondary growth have been proven to be shared across a taxonomically much broader sampling than that considered here (Rothwell et al., 2008).

The placement of *Actinoxylon* as sister to the clade including seed plants and Stenokoleales implies that if *Actinoxylon* was confirmed as an archaeopteridalean progymnosperm, as proposed by Beck (1976), then progymnosperms as a whole would be polyphyletic. However, considering that *Yiduxylon*, a plant that of equivocal taxonomic placement that shares several aneurophyte features, is recovered as sister to the clade including *Actinoxylon*, it is possible that *Actinoxylon*, *Yiduxylon*, and the aneurophyte clade represent a progymnosperm grade at the base of the clade that includes the seed plants and Stenokoleales (Fig. 1). This paraphyletic progymnosperm group could also include *Reimannia*, another putative aneurophyte.

The age of Gensel's (1984) plant, which was dated based on spores (Gensel, 1984), constrains the minimum age of the bilateral clade to the early Emsian (Fig. 1). Although the oldest lignophyte fossil with demonstrated secondary growth, the aneurophyte *Rellimia thomsonii*, may be as old as the late Eifelian (Dannenhofer and Bonamo, 2003), the position of Gensel's (1984) plant as deeply nested within the lignophytes, constrains the minimum age of this clade, as well as that of the aneurophyte ancestor, to the early Emsian. This supports the late Emsian age proposed for what would be the oldest known *Rellimia* (and, by extension, progymnosperm) specimens,

reported from the Devonian of Morocco by Gerrienne et al. (2010). The age of Gensel's (1984) plant also support an early Emsian minimum age for the bilateral clade. The late Emsian *Gothanophyton* constrains the minimum age of Stenokoleales to the Emsian and the position of *Triloboxylon arnoldii* as sister to the seed plants constrains the minimum age of the seed plant ancestor to the Givetian.

1.5. Conclusions and future outlook

We present an updated phylogeny of early euphyllophytes characterized by actinostelic xylem architecture and traditionally associated with the origin of seed plants. We included the most extensive taxon sampling to date, emphasizing anatomically-preserved species. Due to the vagaries of fossil preservation, this broad sampling necessarily constrained the range of informative characters that could be defined (only one on reproductive biology and few on external morphology). We used the resulting set of characters, extensive primarily in terms of vegetative anatomy and including continuous characters, in a maximum parsimony approach. We recovered monophyletic aneurophytes, seed plants, and Stenokoleales, broadly consistent with current taxonomic understanding, although a few species are placed in positions inconsistent with previous taxonomic assignments. These inconsistencies could arise from limitations associated with the number of characters, the structural simplicity of the plants, and our fragmentary knowledge of the species, due to incomplete preservation.

Overall, the aneurophyte clade is sister to the clade including seed plants and Stenokoleales. This topology, (1) places Stenokoleales among the lignophytes, and (2)

indicates that seed plants may share a closer common ancestor with the Stenokoleales than with aneurophyalean progymnosperms. The ages of fossils considered in light of their phylogenetic relationships suggest a Givetian minimum age for the seed plant ancestor, a late Emsian minimum age for the Stenokoleales, and early Emsian minimum ages for lignophytes, the bilateral clade, and the aneurophyte ancestor.

The wealth of detailed information accumulated over more than six decades on the anatomy of early euphyllophytes is starting to bear fruit in terms of assessment of relationships among these plants, which were previously based on taxonomic decisions derived from comparative approaches only. Our study is the first to explore empirically (i.e. in a phylogenetic context) patterns of relationships among a broad sampling of species associated with the origin of seed plants. The results are encouraging for resolution of relationships among early euphyllophytes that include the seed plant ancestor. They also indicate some gaps in our knowledge, suggesting directions for further exploration. Thus, additional discoveries are needed to understand the detailed anatomy of some incompletely characterized species, as well as to increase knowledge of the morphology of many of these species (e.g., branching architecture). Such new information on the anatomy and morphology of incompletely characterized species would increase the number of characters and significantly decrease the amount of missing data.

Likewise, documentation of the reproductive structures for more of these species is bound to improve phylogenetic resolution. For instance, of the nine seed plant species included here, only one (*Elkinsia*) is known with attached reproductive structures (ovules), whereas the others are assumed to be seed plants based on similarities in

vegetative anatomy. In the same way, all *Stenokoleales* are known exclusively from vegetative permineralized axes, as are the species of uncertain taxonomic affinities, *Langoxylon asterochlaenoideum*, *Gothanophyton zimmemanni*, and Gensel's (1984) plant. The last two are the only two actinostelic euphyllophytes currently known from the Early Devonian (Emsian) and suggest that the Early Devonian could reveal additional euphyllophyte diversity relevant to the questions addressed here. This calls for renewed efforts to extend sampling deeper in the Devonian, in order to discover and characterize new anatomically-preserved euphyllophytes, particularly from the Emsian-Givetian interval.

Finally, it will be interesting to see how inclusion of cladoxyloids and archaeopteridalean progymnosperms influence hypotheses of relationships when included in phylogenetic analyses. Cladoxyloids, including the iridopterids and pseudosporochnaleans, are interesting because they form another major group of euphyllophytes that was diverse during the Devonian, and some are characterized by actinosteles, although their "permanent protoxylem" architecture (Beck and Stein, 1993) is different from that of most of the plants discussed here.

Perhaps most importantly, archaeopteridalean progymnosperms are interesting because they are the only tracheophyte group that possesses eusteles, other than seed plants, which are in their majority, and in exclusivity for modern floras, represented by eustelic forms. Thus, whereas archaeopterids, eustelic and heterosporous, resemble more closely the modern seed plants, the actinostelic aneurophytes are more similar to the oldest known seed plants. These patterns of similarity have generated competing

hypotheses for the origins of seed plants. The hypotheses were reviewed by Rothwell and Erwin (1987), who argued for closer relationships between seed plants and aneurophytes, and not archaeopterids. Considering that (1) protostelic organization is plesiomorphic among euphyllophytes; (2) most plant groups (and satellite taxa) included in discussions of seed plant origins are protostelic; and (3) archaeopterids and the eustelic architecture are younger (Givetian) as compared to a majority of the plants in the plexus of seed plant precursor taxa, we agree with the views of Rothwell and Erwin (1987), hence our taxon selection for this study. These implications are somewhat weakened by the absence of direct evidence pointing to heterospory in the aneurophytes, although much is left to be discovered about the reproductive biology of this group. Ultimately, resolution of relationships between seed plants, actinostelic aneurophytalan progymnosperms resembling the earliest seed plants, and eustelic archaeopterids resembling extant seed plants, along with Stenokoleales and satellite taxa of all these major groups, will require broadening of the dataset used here to include archaeopterids. This will necessitate addition of a well-thought and thoroughly justified set of characters, along with modification of some of the characters used in this study, to code for the eustelic condition within a framework that allows for hypothesis testing. These are no trivial tasks and will require significant reflection, but such a study is bound to provide interesting answers on the evolution of stelar architecture in the lignophyte clade, and on the evolution of seed plants, in general.

Literature cited

- BANKS, H. P., S. LECLERCQ, AND F. M. HUEBER. 1975. Anatomy and morphology of *Psilophyton dawsonii*, sp. n. from the later Lower Devonian of Quebec (Gaspé), and Ontario, Canada. *Palaeontographica Americana* 48: 75–127.
- BAPST, D. W. 2012. Paleotree: an R package for paleontological and phylogenetic analyses of evolution. *Methods in Ecology and Evolution* 3: 803–807.
- BARNARD, P. D. W., AND A. G. LONG. 1974. *Triradioxylon* – a new genus of Lower Carboniferous petrified stems and petioles together with a review of the classification of early Pteridophytina. *Transactions of the Royal Society of Edinburgh* 69: 231–249.
- BATEMAN, R. M., P. R. CRANE, W. A. DiMICHELE, P. KENRICK, N. P. ROWE, T. SPECK, AND W. E. STEIN. 1998. Early evolution of land plants: phylogeny, physiology, and ecology of the primary terrestrial radiation. *Annual Reviews of Ecology and Systematics* 29: 263–292.
- BECK, C. B. 1957. *Tetraxylopteris schmidtii* gen. et sp. nov., a probable pteridosperm precursor from the Middle Devonian of New York. *American Journal of Botany* 44: 350–367.
- BECK, C. B. 1960a. The identity of the *Archaeopteris* and *Callixylon*. *Brittonia* 12: 351–368.
- BECK, C. B. 1960b. Studies of New Albany Shale plants. I. *Stenokoleos simplex* comb. nov. *American Journal of Botany* 47: 115–124.
- BECK, C. B. 1976. Current status of the Progymnospermopsida. *Review of Palaeobotany and Palynology* 21: 5–23.
- BECK, C. B., AND W. E. STEIN. 1993. *Crossia virginiana* gen. et sp. nov., a new member of the Stenokoleales from the Middle Devonian of southwestern Virginia. *Palaeontographica B* 29: 115–134.

- BELL, M. A., AND G. T. LLOYD. 2015. strap: an R package for plotting phylogenies against stratigraphy and assessing their stratigraphic congruence. *Palaeontology* 58: 379–389.
- BENKOVÁ E, M. MICHNIEWICZ, M. SAUER, T. TEICHMANN, D. SEIFERTOVA, G. JURGENS, AND J. FRIML. 2003. Local, efflux-dependent auxin gradients as a common module for plant organ formation. *Cell* 115: 591–602.
- BERTRAND, P. 1941. Anatomie comparée des Pteridospermes et des Filicales primitives. *Comptes rendus hebdomadaires des séances de l'Académie des Sciences* 213: 143–145.
- BONAMO, P. M. 1975. The Progymnospermopsida: building a concept. *Taxon* 24: 569–579.
- BONAMO, P. M. 1977. *Rellimia thomsonii* (Progymnospermopsida) from the Middle Devonian of New York State. *American Journal of Botany* 64: 1272–1285.
- CORNET, L., P. GERRIENNE, B. MEYER-BERTHAUD, AND C. PRESTIANNI. 2012. A Middle Devonian *Callixylon* (Archaeopteridales) from Ronquières, Belgium. *Review of Palaeobotany and Palynology* 183: 1–8.
- DANNENHOFFER, J. M., AND P. M. BONAMO. 2003. The wood of *Rellimia* from the Middle Devonian of New York. *International Journal of Plant Sciences* 164: 429–441.
- DANNENHOFFER, J. M., W. STEIN, AND P. M. BONAMO. 2007. The primary body of *Rellimia thomsonii*: integrated perspective based on organically connected specimens. *International Journal of Plant Sciences* 168: 491–506.
- DUNN, M. T., AND G. W. ROTHWELL. 2012. Phenotypic plasticity of the hydrasperman seed fern *Tetrastichia bupatides* Gordon (Lyginopteridaceae). *International Journal of Plant Sciences* 173: 823–834.
- ESCAPA, I. H., AND D. POL. 2011. Dealing with incompleteness: new advances for the use of fossils in phylogenetic analysis. *Palaios* 26: 121–124.
- GALTIER, J. 1977. *Tristichia longii*, nouvelle pteridosperme probable du Carbonifère de la Montagne Noire. *Comptes rendus hebdomadaires des séances de l'Académie des Sciences* 284: 2215–2218.

- GALTIER, J., AND B. MEYER-BERTHAUD. 1996. The early seed plant *Tristichia tripus* (Unger) comb. nov. from the Lower Carboniferous of Saalfeld, Thuringia. *Review of Palaeobotany and Palynology* 93: 299–315.
- GENSEL, P. G. 1984. A new Lower Devonian plant and the early evolution of leaves. *Nature* 309: 785–787.
- GERRIENNE, P., B. MEYER-BERTHAUD, H. LARDEUX, AND S. REGNAULT. 2010. First record of *Rellimia* Leclercq & Bonamo (Aneurophytales) from Gondwana, with comments on the earliest lignophytes. In M. Vecoli, G. Clement, and B. Meyer-Berthaud [eds], *The terrestrialization process: modelling complex interactions at the biosphere-geosphere interface*, 81–92. The Geological Society, London, UK.
- GOLOBOFF, P. A., AND S. A. CATALANO. 2016. TNT version 1.5, including a full implementation of phylogenetic morphometrics. *Cladistics* 32: 221–238.
- HARTMAN, C. M., AND H. P. BANKS. 1980. Pitting in *Psilophyton dawsonii*, an Early Devonian trimerophyte. *American Journal of Botany* 67: 400–412.
- HILTON, J., AND R. M. BATEMAN. 2006. Pteridosperms are the backbone of seed-plant phylogeny. *Journal of the Torrey Botanical Society* 133: 119–168.
- HOSKINS, C. H., AND A. T. CROSS. 1951. The structure and classification of four plants from the New Albany Shale. *American Midland Naturalist* 46: 684–716.
- KENRICK, P., AND P. R. CRANE. 1997. *The origin and early diversification of land plants*. Smithsonian Institution Press, Washington.
- KLAVINS, S. D., AND L. C. MATTEN. 1996. Reconstruction of the frond *Laceyia hibernica*, a lyginopterid pteridosperm from the uppermost Devonian of Ireland. *Review of Palaeobotany and Palynology* 93: 253–268.
- LENHARD, M. 2017. Plant development: Keeping on the straight and narrow and flat. *Current Biology* 27: R1277–R1280.
- LONG, A. G. 1961. *Tristichia ovensi* gen. et sp. nov., a protostelic Lower Carboniferous pteridosperm from Berwickshire and East Lothian, with an account of some associated seeds and cupules. *Transactions of the Royal Society of Edinburgh* 64: 477–489.

- LONG, A. G. 1976. *Calathopteris heterophylla* gen. et sp. nov., a Lower Carboniferous pteridosperm bearing two kinds of petioles. *Transactions of the Royal Society of Edinburgh* 13: 327–336.
- MADDISON, W. P., AND D. R. MADDISON. 2009. Mesquite: a modular system for evolutionary analysis. Version 3.2. <http://mesquiteproject.org>.
- MATTEN, L. C. 1968. *Actinoxylon banksii* gen. et sp. nov.: a progymnosperm from the Middle Devonian of New York. *American Journal of Botany* 55: 773–782.
- MATTEN, L. C. 1973. The Cairoa Flora (Givetina) of eastern New York. I. *Reimannia terete* axes, and *Cairoa lamanekii* gen. et sp. n. *American Journal of Botany* 60: 619–630.
- MATTEN, L. C. 1992. Studies on Devonian plants from New York State: *Stenokoleos holmesii* n. sp. from the Cairo Flora (Givetian) with an alternative model for lyginopterid seed fern evolution. *Courier Forschungs-Institut Senckenberg* 147: 75–85.
- MATTEN, L. C., AND H. P. BANKS. 1966. *Triloboxylon ashlandicum* gen. and sp. n. from the Upper Devonian of New York. *American Journal of Botany* 53: 1020–1028.
- MATTEN, L. C., AND H. P. BANKS. 1969. *Stenokoleos bifidus* sp. n. in the Upper Devonian of New York State. *American Journal of Botany* 56: 880–891.
- MAY, B. I., AND L. C. MATTEN. 1983. A probable pteridosperm from the uppermost Devonian near Ballyheigue, Co. Kerry, Ireland. *Botanical Journal of the Linnean Society* 86: 103–123.
- MOMONT, N. 2015. Investigation of basal lignophytes: the Aneurophytales and the Stenokoleales re-examined. Ph. D. dissertation, University of Liège, Liège, Belgium.
- MOMONT, N., A. DECOMBEIX, P. GERRIENNE, AND C. PRESTIANNI. 2016a. New information, including anatomy of the secondary xylem, on the genus *Brabantophyton* (Stenokoleales) from Ronquières (Middle Devonian, Belgium). *Review of Palaeobotany and Palynology* 234: 44–60.

- MOMONT, N., P. GERRIENNE, AND C. PRESTIANNI. 2016b. *Brabantophyton*, a new genus with stenokolealean affinities from a Middle to earliest Upper Devonian locality from Belgium. *Review of Palaeobotany and Palynology* 227: 77–96.
- PRESTIANNI, C., AND P. GERRIENNE. 2010. Early seed plant radiation: an ecological hypothesis. In M. Vecoli, G. Clement, and B. Meyer-Berthaud [eds], *The terrestrialization process: modelling complex interactions at the biosphere-geosphere interface*, 71–80. The Geological Society, London, UK.
- R CORE TEAM. 2017. R: a language and environment for statistical computing. v. 3.4.1. *R Foundation for Statistical Computing*. [WWW document] URL <https://r-project.org>. [accessed 11.01.2017].
- REMY, W., AND H. HASS. 1986. *Gothanophyton zimmermanni* nov. gen. nov. spec., eine Pflanze mit komplexem stellar Körper aus dem Emsian. *Argumenta Palaeobotanica* 7: 9–69.
- ROTHWELL, G. W., AND D. M. ERWIN. 1987. Origin of seed plants: an aneurophyte/seed-fern link elaborated. *American Journal of Botany* 74: 970–973.
- ROTHWELL, G. W., H. SANDERS, S. E. WYATT, AND S. LEV-YADUN. 2008. A fossil record for growth regulation: the role of auxin in wood evolution. *Annals of the Missouri Botanical Garden* 95: 121–134.
- ROTHWELL, G. W., S. E. SCHECKLER, AND W. H. GILLESPIE. 1989. *Elkinsia* gen. et sp. nov., a Late Devonian gymnosperm with cupulate ovules. *Botanical Gazette* 158: 170–189.
- ROTHWELL, G. W., AND R. SERBET. 1994. Lignophyte phylogeny and the evolution of spermatophytes: a numerical cladistics analysis. *Systematic Botany* 19: 443–482.
- SANDERS, H., G. W. ROTHWELL, AND S. E. WYATT. 2007. Paleontological context for the developmental mechanisms of evolution. *International Journal of Plant Sciences* 168: 719–728.
- SCHECKLER, S. E. 1976. Ontogeny of progymnosperms. I. Shoots of Upper Devonian Aneurophytales. *Canadian Journal of Botany* 54: 202–219.

- SCHECKLER, S. H., AND H. P. BANKS. 1971a. Anatomy and relationships of some Devonian progymnosperms from New York. *American Journal of Botany* 58: 737–751.
- SCHECKLER, S. H., AND H. P. BANKS. 1971b. *Proteokalon* a new genus of progymnosperms from the Devonian of New York State and its bearing on phylogenetic trends in the group. *American Journal of Botany* 58: 874–884.
- SCHECKLER, S. E., J. E. SKOG, AND H. P. BANKS. 2006. *Langoxylon asterochlaenoideum* Stockmans: Anatomy and relationship of a fern-like plant from the Middle Devonian of Belgium. *Review of Palaeobotany and Palynology* 142: 193–217.
- SCHWEITZER, H. J., AND L. C. MATTEN. 1982. *Aneurophyton germanicum* and *Protopteridium thomsonii* from the Middle Devonian of Germany. *Palaeontographica B* 184: 65–106.
- SERBET, R., AND G. W. ROTHWELL. 1992. Characterizing the most primitive seed ferns. I. A reconstruction of *Elkinsia polymorpha*. *International Journal of Plant Sciences* 153: 602–621.
- SERLIN, B. S., AND H. P. BANKS. 1978. Morphology and anatomy of *Aneurophyton*, a progymnosperm from the Late Devonian of New York. *Palaeontographica Americana* 51: 47–51.
- STEIN, W. E. 1982. The Devonian plant *Reimannia*, with a discussion of the class Progymnospermopsida. *Palaeontology* 25: 605–622.
- STEIN, W. E., AND C. B. BECK. 1983. *Triloboxylon arnoldii* from the Middle Devonian of western New York. *Contributions from the Museum of Paleontology* 26: 257–288.
- WANG, D., AND L. LIU. 2015. A new Late Devonian genus with seed plant affinities. *BMC Evolutionary Biology* 28: 1–16.

Figures

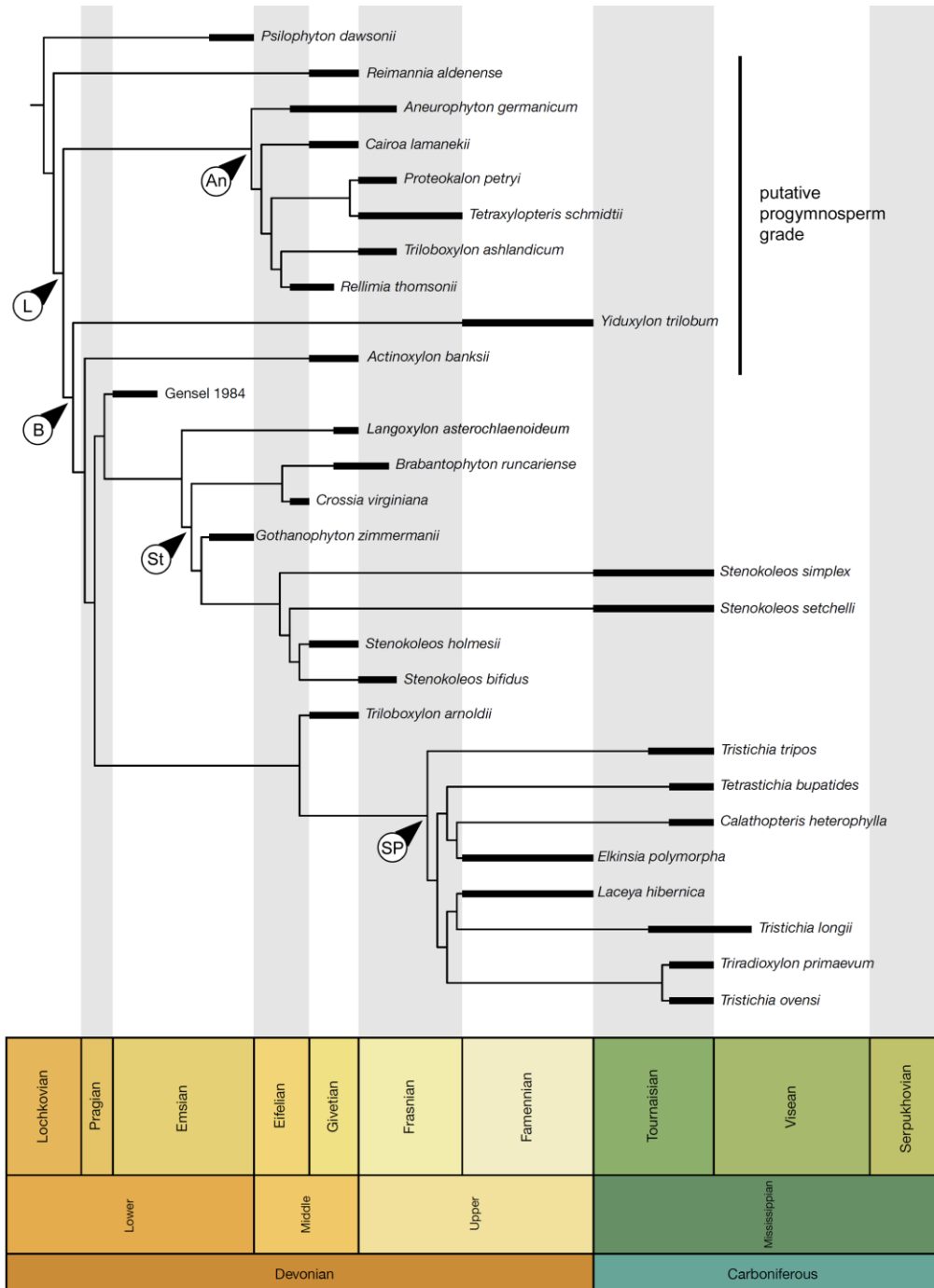


Figure 1 Time-calibrated single MP tree of 96.33 steps (CI = 0.528, RI = 0.656) resulting from Analysis 2, using discrete and continuous characters. Thick bars indicate published

ages of each species. Clades are labeled An = aneurophyte clade; B = bilateral clade; L = lignophytes; SP = seed plant clade; St = Stenokoleales clade.

Appendix A

Taxa used in the analyses.

Actinoxylon banksii (Archaeopteridales), Givetian, Kiskatam Formation (USA), based on Matten (1968), Beck (1976), and Cornet et al. (2012)

Aneurophyton germanicum (Aneurophytales), Givetian - Frasnian, Delaware River Formation (USA), Honsel Formation (Germany), based on Serlin and Banks (1978) and Schweitzer and Matten (1982)

Brabantophyton runcariense (Stenokoleales), Givetian - Frasnian, Bois de Bordeaux Formation (Belgium), based on Momont et al. (2016a, b)

Cairoa lamanekii (Aneurophytales), Givetian, Plattkill Formation (USA), based on Matten (1973)

Calathopteris heterophylla (seed plant), Upper Tournaisian, Cementstone Group (Scotland), based on Long (1976)

Crossia virginiana (Stenokoleales), Middle Devonian, Milboro Shale (USA), based on Beck and Stein (1993)

Elkinsia polymorpha (seed plant), Famennian, Upper Hampshire Formation (USA), based on Rothwell et al. (1989) and Serbet and Rothwell (1992)

Gensel 1984 (*Incertae sedis*), Emsian, Battery Point Formation (Canada), based on Gensel (1984)

Gothanophyton zimmermanni (*Incertae sedis*), Emsian (Rheinischen Schiefergebirges, Germany), based on Remy and Hass (1986), Scheckler et al. (2006), and Momont et al. (2016b)

Laceyia hibernica (seed plant), Upper Devonian, Coomhola Formation (Ireland), based on May and Matten (1983) and Klavins and Matten (1996)

Langoxylon asterochlaenoideum (*Incertae sedis*), Givetian, Bois de Bordeaux Formation (Belgium), based on Scheckler et al. (2006)

Proteokalon petryi (Aneurophytales), Frasnian, Oneonta Formation (USA), based on Scheckler and Banks (1971b) and Scheckler (1976)

Psilophyton dawsonii (Trimerophytina), Emsian, Sextant Formation and Battery Point Formation (Canada), based on Banks et al. (1975) and Hartman and Banks (1980)

Reimannia aldenense (Aneurophytales), Givetian, Ludlowville Formation, Plattekill Formation (USA), based on Matten (1973) and Stein (1982)

Rellimia thomsonii (Aneurophytales), Eifelian - Givetian, Panther Mountain Formation (USA), based on Bonamo (1977), Dannenhoffer and Bonamo (2003), and Dannenhoffer et al. (2007)

Stenokoleos bifidus (Stenokoleales), Frasnian, Oneonta Formation (USA), based on Matten and Banks (1969)

Stenokoleos holmesii (Stenokoleales), Givetian, Kiskatom Formation (USA), based on Matten (1992)

Stenokoleos setchelli (Stenokoleales), Mississippian, Sanderson Formation (USA), based on Beck (1960b)

Stenokoleos simplex (Stenokoleales), Upper Devonian - Tournaisian, Sanderson Formation (USA), based on Hoskins and Cross (1951) and Beck (1960b)

Tetrastichia bupatides (seed plant), Tournaisian, Lower Lothian Group, Calciferous Sandstone Series (Scotland), based on Bertrand (1941) and Dunn and Rothwell (2012)

Tetraxylopteris schmidtii (Aneurophytales), Frasnian, Oneonta Formation (USA), based on Beck (1957) and Scheckler and Banks (1971a)

Triloboxylon ashlandicum (Aneurophytales), Frasnian, Oneonta Formation (USA), based on Matten and Banks (1966) and Scheckler and Banks (1971a)

Triloboxylon arnoldii (Aneurophytales), Givetian, Ludlowville Formation (USA), based on Stein and Beck (1983).

Triradioxylon primaevum (seed plant), Tournaisian, Calciferous Sandstone Series, Cementstone Group (Scotland), based on Barnard and Long (1974)

Tristichia longii (seed plant), Tournaisian, Horizon des lydiennes (France) and Germany, based on Galtier (1977) and Galtier and Meyer-Berthaud (1996)

Tristichia ovensi (seed plant), Tournaisian, Calciferous Sandstone Series, Cementstone Group (Scotland) and Germany, based on Long (1961) and Galtier and Meyer-Berthaud (1996)

Tristichia tripos (seed plant), Tournaisian, Russchiefer (Germany), based on Galtier and Meyer-Berthaud (1996)

Yiduxylon trilobum (seed plant), Famennian, Tizikou Formation (China), based on Wang and Liu (2015)

Appendix B
Characters used in the analyses.

Continuous characters

0. Maximum primary xylem diameter:maximum axis diameter (ratio)

We used primarily information from the literature for both maximum primary xylem diameter and maximum axis diameter. For those species with no explicit listing of sizes, we took measurements from the published illustration. The maximum primary xylem diameter was obtained by doubling the distance measured from the center of the stele to the tip of the longest primary xylem rib. For the maximum axis diameter, we measured the longest distance that crossed the center of the axis.

1. Primary xylem surface area:overall surface area of axis, in cross section (ratio)

For these measurements we used the published illustration and selected the lowest order of branching.

2. Maximum depth of primary xylem lobes/ribs, in cross section (lobe length:xylem radius; ratio)

For xylem lobe (rib) length, we measured the distance between the tip and the basalmost point of this lobe the longest xylem lobe was chosen. For the xylem radius we used the maximum radius as measured for character 7.

3. Primary xylem lobe basal width:max xylem diameter, in cross section (ratio)

This character was estimated by measuring the width of the thickest primary xylem lobe at the base and the maximum diameter of the primary xylem, as measured for character 7.

4. Maximum metaxylem tracheid diameter (in radial organographic domain)

5. Maximum diameter of secondary xylem tracheids

6. Axis width ratio at transition from radial to bilateral symmetry in branching system (R:B diameter)

7. Maximum metaxylem tracheid diameter (in bilateral organographic domain)

8. Maximum diameter of recurring appendages with terete xylem

Discrete characters

9. Life cycle

0 = homosporous; 1 = heterosporous

10. Bilateral organographic domain

0 = absent; 1 = present

Radial and bilateral symmetry are assessed based on the symmetry of the primary xylem as seen in transverse section. All taxa included exhibit radial symmetry in axes of the lower orders of branching; together, these are referred to as the *radial organographic domain*. In some of the taxa, higher orders of branching exhibit bilateral symmetry and these form the *bilateral organographic domain*.

Characters 10-36 and 41-48 do not apply to higher orders of branching with terete xylem, which are treated separately as *recurring appendages with terete xylem* (characters 37-40).

11. Number of anatomically distinct orders of branching in the radial organographic domain

1; 2; 3 ...

This character refers to differences in the anatomy of axes that exhibit radial symmetry. These are usually differences in number of xylem ribs/lobes. Taxa in which all orders of branching in the radial organographic domain have identical anatomy are scored "1".

12. Branching architecture of radial organographic domain

0 = irregular; 1 = alternate; 2 = sub-opposite

This character refers to the taxis of axes of the N (that belongs to the radial or bilateral domain) branching order on the subtending N-1 axes (that belongs to the radial domain). Alternate taxis (1) refers exclusively to regular helical taxis.

13. Number of ranks in the taxis of branching of the radial organographic domain.

2; 3; 4 ...

This character only applies to those taxa which have (1) alternate or (2) sub-opposite branching architecture. The number of ranks was scored based on the information in the literature or deduced indirectly from the number of ridges of the stele in the radial domain that supplied traces to these branches.

14. Primary xylem cross-sectional outline (radial organographic domain)

0 = circular; 1 = lobed/ribbed

15. Number of primary xylem lobes/ribs (radial organographic domain)

3; 4 ...

This character can be polymorphic, as axes of different sizes or of different orders of branching can have different numbers of primary xylem lobes, in the same species. Because in many taxa it is not known whether the largest axes described are main upright axes or side branches and, therefore, it is impossible to homologize orders of branching between taxa, this character collapses all known orders of branching (of the radial organographic domain).

16. Primary xylem lobe branching

0 = absent; 1 = present

This character refers to the ribs (lobes) of actinosteles that bifurcate producing secondary lobes in transverse section (e.g., *Brabantophyton*; Momont et al. 2016b).

17. Central protoxylem strand

0 = absent; 1 = present

This character refers to the presence of a protoxylem strand that is located at the center of the stele.

18. Protoxylem strands at rib midplane

0 = absent; 1 = present

This character refers to the presence of protoxylem strands along the ribs (between the center of the stele and the tip of the rib)

19. Protoxylem architecture (for taxa with more than a single central protoxylem strand)

0 = permanent; 1 = radiate

This character refers to the pattern in which protoxylem strands originate and branch vertically, along an axis (i.e. Beck and Stein, 1993). (0 = permanent) There is no central protoxylem strand from which all other strands diverge, each protoxylem strand is independent; (1 = radiate) There is only a single central protoxylem strand from which all other strands (i.e. at rib midplanes) originate.

20. Protoxylem lacunae (i.e., rhexigenous, with remnants of annular/helical secondary wall thickenings, or lysigenous)

0 = absent; 1 = present

Protoxylem lacunae are defined here as an open area or a physical gap present in the place of peripheral protoxylem strands. This is not associated with a hypothesis on their specific mode of development, i.e., rhexigenous vs. lysigenous. Nevertheless, this is different from the open areas formed by the incomplete preservation of protoxylem parenchyma, which is a different character (character 21).

21. Protoxylem parenchyma

0 = absent; 1 = present

22. Smaller, radially-elongated metaxylem connecting protoxylem strands along rib midplanes (in cross section)

0 = absent; 1 = present discontinuously; 2 = present, continuous

This character refers to the presence of small sized metaxylem tracheids that are elongated radially and connect adjacent protoxylem strands along the xylem rib.

23. Metaxylem parenchyma

0 = absent; 1 = present

24. Metaxylem tracheid pitting
0 = P-type thickenings; 1 = circular bordered pits
25. Multiseriate pitting of metaxylem tracheid walls
0 = alternate; 1 = opposite
26. Secondary xylem
0 = absent; 1 = present
27. Secondary xylem tracheid pitting
0 = P-type thickenings; 1 = circular bordered pits
28. Xylem rays
0 = absent; 1 = present
29. Scattered sclerenchyma in cortex (other than outer cortex)
0 = absent; 1 = present
This character refers to the presence of sclerenchyma cells with no consistent distribution/positioning clusters that are distributed in a specific and consistent way in the cortex (exclusive of the outer cortex region).
30. Consistently organized sclerenchyma in cortex (other than outer cortex)
0 = absent; 1 = present
This character refers to the presence of sclerenchyma cell clusters that are distributed in a specific and consistent way in the cortex (exclusive of the outer cortex region).
31. Secretory cells in cortex
0 = absent; 1 = present
This character refers to the presence of cells that have dark content but no thickened walls.
32. Outer cortex
0 = parenchymatous; 1 = with significant and consistent sclerenchyma content
33. Sclerenchyma in outer cortex
0 = continuous layer; 1 = heterogeneous *Sparganum*-type; 2 = heterogeneous *Dictyoxylon*-type
This character refers to the distribution of sclerenchymatous tissue in the outer cortex of orders of branching that belong to the radial domain. (0) refers to a continuous layer of sclerenchyma; (1) refers to a layer consisting of groups of sclerenchyma that alternate with parenchyma (in cross section), while forming parallel non-anastomosing strands

vertically; (2) refers to a layer consisting of groups of sclerenchyma that alternate with parenchyma (in cross section), while also anastomosing longitudinally.

34. Capitulate glands

0 = absent; 1 = present

This character refers to the presence on the epidermis of trichomes that have an expanded apex.

35. Direction of trace divergence to next order of branching (between branching orders of the radial organographic domain)

0 = radial; 1 = tangential

This character refers to the direction in which traces depart, with respect to the actinostele rib from which they originate.

36. Pulvinus-like base of branches (radial or bilateral)

0 = absent; 1 = present

This character refers to the presence of branches with an expanded basal part.

37. Recurring appendages with terete xylem

0 = absent; 1 = present

This character refers to higher (highest) orders of branching that possess terete xylem strands. These are found in appendages that are repeated as modules along lower order axes. Such appendages have determinate growth in all cases where enough evidence is available.

38. Taxis of recurring appendages with terete xylem

0 = irregular; 1 = alternate; 2 = sub-opposite

This character refers to the arrangement of the recurring appendages with terete xylem on branches of the subtending order of branching.

39. Dissection of recurring appendages with terete xylem

0 = isotomous; 1 = anisotomous

40. Architecture of recurring appendages with terete xylem

0 = three-dimensional; 1 = planar

41. Direction of trace divergence from radial to bilateral organographic domain

0 = radial; 1 = tangential

This character refers to the direction in which traces depart, with respect to the actinostele rib from which they originate, at the transition from the highest order of branching in the radial domain to the lowest (first) order of branching in the bilateral domain.

42. Number of vascular bundles in traces diverging from radial to bilateral organographic domain

0 = one; 1 = more than one

This character refers to the number of vascular bundles that depart from the tip of a xylem rib during at branching from the highest order of branching of the radial domain to the lowest (first) order of branching in the bilateral domain.

43. Branching of initial trace(s) before entering the base of the bilateral appendage

0 = absent; 1 = present

This character refers to whether the bundles that diverge initially from the tip of the xylem rib split further into more vascular bundles before entering the base of the branch.

44. Adaxial-abaxial asymmetry of the vascular supply of the bilateral organographic domain

0 = absent; 1 = present

This character is based on the cross-sectional shape of the trace supplying the lowest order of branching in the bilateral organographic domain. If the adaxial side of the trace is symmetrical to the abaxial side, the character is scored (0). If there is any kind of asymmetry between the two sides (e.g., protoxylem strands only toward adaxial side of the trace or concave adaxial side vs. convex abaxial side) the character is scored (1).

45. Branching architecture of bilateral organographic domain

0 = irregular; 1 = alternate; 2 = sub-opposite; 3 = bipartite

This character refers to the taxis of axes of the N branching order (regardless of having radial or bilateral symmetry) on the subtending N-1 axes (which belongs to the bilateral domain). Bipartite refers to the condition present in *Stenokoleales*, in which the axes of the bilateral domain bifurcate at the base.

46. Number of ranks in branch taxis of bilateral organographic domain

2; 3; 4 ...

This character only applies to taxa which were scored as (1) or (2) in the previous character. Taxa were scored based on information provided in the literature (either explicitly mentioned in the text or shown in illustrations). For the taxa that have planar branching on the bilateral domain (i.e.: seed plants), the number of rank was scored as 2.

47. Outer cortex in appendages of bilateral organographic domain

0 = parenchymatous; 1 = with significant sclerenchyma content

This character refers to the cell type that dominates the outer cortex region in the orders of branching that belong to the bilateral domain.

48. Sclerenchyma in outer cortex (appendages of bilateral organographic domain)

0 = continuous layer; 1 = heterogeneous *Sparganum*-type; 2 = heterogeneous *Dictyoxylon*-type

See Character 33.

Appendix C
Character Scoring

Table 1 Continuous character scoring 1

Character	0. Max primary xylem diameter : max axis diameter					1. Primary xylem surface area : axis overall surface area (cross section)					2. Maximum depth of primary xylem lobes (lobe length : xylem radius)				
	measure	min	max	stand min	stand max	measure	min	max	stand min	stand max	measure	min	max	stand min	stand max
<i>Psilophyton dawsonii</i>	0.41	0.37	0.45	0.37	0.45	0.12	0.10	0.13	0.23	0.28	-	-	-	-	-
<i>Stenokoleos simplex</i>	0.47	0.42	0.51	0.42	0.51	0.11	0.10	0.12	0.22	0.26	0.53	0.48	0.25	0.37	0.45
<i>Stenokoleos bifidus</i>	0.68	0.61	0.75	0.61	0.75	0.21	0.19	0.23	0.41	0.50	0.48	0.43	0.45	0.67	0.82
<i>Stenokoleos holmesii</i>	0.60	0.54	0.66	0.54	0.66	0.32	0.29	0.36	0.63	0.77	0.68	0.61	0.55	0.82	1.00
<i>Stenokoleos setchelli</i>	0.90	0.81	0.99	0.81	0.99	0.18	0.16	0.20	0.35	0.43	0.83	0.75	0.29	0.43	0.53
<i>Crossia virginiana</i>	0.77	0.69	0.85	0.69	0.85	0.33	0.30	0.37	0.65	0.80	0.76	0.69	0.51	0.76	0.92
<i>Brabantophyton runcariense</i>	0.80	0.72	0.88	0.72	0.88	0.42	0.38	0.46	0.83	1.00	0.82	0.74	0.23	0.33	0.41
<i>Cairoa lamanekii</i>	0.21	0.19	0.23	0.19	0.23	0.12	0.11	0.13	0.24	0.29	0.81	0.73	0.20	0.30	0.37
<i>Rellimia thomsonii</i>	0.91	0.82	1.00	0.82	1.00	0.11	0.10	0.12	0.22	0.26	0.86	0.78	0.12	0.18	0.22
<i>Reimannia aldenense</i>	0.34	0.31	0.37	0.31	0.37	0.06	0.05	0.06	0.11	0.14	0.74	0.67	0.12	0.18	0.22
<i>Tetraxylopteris schmidtii</i>	0.04	0.03	0.04	0.03	0.04	0.15	0.13	0.16	0.29	0.35	0.88	0.79	0.13	0.19	0.23
<i>Aneurophyton germanicum</i>	0.38	0.34	0.42	0.34	0.42	0.17	0.15	0.19	0.33	0.40	0.80	0.72	0.25	0.37	0.45
<i>Proteokalon petryi</i>	0.60	0.54	0.66	0.54	0.66	0.08	0.08	0.09	0.17	0.20	0.71	0.64	0.12	0.18	0.21
<i>Triloboxylon ashlandicum</i>	0.48	0.43	0.53	0.43	0.53	0.13	0.12	0.15	0.26	0.32	0.80	0.72	0.09	0.14	0.17
<i>Triloboxylon arnoldii</i>	0.47	0.42	0.51	0.42	0.51	0.02	0.02	0.03	0.05	0.06	0.73	0.65	0.17	0.26	0.32
<i>Actinoxylon banksii</i>	0.50	0.45	0.55	0.45	0.55	?	?	?	?	?	0.65	0.58	0.31	0.46	0.56
Gensel (1984) euphyllophyte	0.70	0.63	0.77	0.63	0.77	0.34	0.30	0.37	0.66	0.81	0.87	0.78	0.15	0.22	0.26
<i>Gothanophyton zimmermanni</i>	0.88	0.79	0.96	0.79	0.96	0.34	0.31	0.38	0.67	0.82	0.73	0.66	0.06	0.09	0.11
<i>Elkinsia polymorpha</i>	0.54	0.49	0.60	0.49	0.60	0.22	0.20	0.24	0.44	0.53	0.83	0.74	0.23	0.34	0.42
<i>Tetrastichia bupatides</i>	0.35	0.32	0.39	0.32	0.39	0.04	0.04	0.05	0.09	0.11	0.70	0.63	0.17	0.25	0.30
<i>Tristichia tripos</i>	0.43	0.38	0.47	0.38	0.47	0.10	0.09	0.11	0.20	0.25	0.96	0.87	0.45	0.67	0.82
<i>Tristichia ovensi</i>	0.13	0.11	0.14	0.11	0.14	0.07	0.06	0.08	0.13	0.16	0.86	0.77	0.16	0.23	0.29
<i>Tristichia longii</i>	0.38	0.35	0.42	0.35	0.42	0.09	0.08	0.10	0.18	0.22	0.68	0.61	0.30	0.44	0.54
<i>Laceyia hibernica</i>	0.30	0.27	0.33	0.27	0.33	0.09	0.08	0.10	0.18	0.22	0.80	0.72	0.39	0.57	0.70
<i>Yiduxylon trilobum</i>	0.29	0.26	0.31	0.26	0.31	0.03	0.02	0.03	0.05	0.06	?	?	?	?	?
<i>Calathopteris heterophylla</i>	0.75	0.68	0.83	0.68	0.83	0.13	0.12	0.14	0.25	0.31	?	?	?	?	?
<i>Langoxylon asterochlaenoideum</i>	0.46	0.42	0.51	0.42	0.51	0.20	0.18	0.22	0.39	0.47	0.73	0.65	0.33	0.49	0.60
<i>Triradioxylon primaevum</i>	0.13	0.11	0.14	0.11	0.14	0.04	0.04	0.05	0.08	0.10	?	?	?	?	?

Appendix C (continued)

Table 1 Continuous character scoring 2

Character	3. Primary xylem lobe basal width : max xylem diameter					4. Max metaxylem tracheid diameter (µm)					5. Max secondary xylem tracheid diameter (µm)				
	measure	min	max	stand min	stand max	measure	min	max	stand min	stand max	measure	min	max	stand min	stand max
<i>Psilophyton dawsonii</i>	-	-	-	-	-	80.00	72.00	88.00	0.52	0.63	-	-	-	-	-
<i>Stenokoleos simplex</i>	0.23	0.20	0.25	0.37	0.45	58.00	52.20	63.80	0.38	0.46	-	-	-	-	-
<i>Stenokoleos bifidus</i>	0.41	0.37	0.45	0.67	0.82	100.00	90.00	110.00	0.65	0.79	-	-	-	-	-
<i>Stenokoleos holmesii</i>	0.50	0.45	0.55	0.82	1.00	77.00	69.30	84.70	0.50	0.61	-	-	-	-	-
<i>Stenokoleos setchelli</i>	0.27	0.24	0.29	0.43	0.53	55.00	49.50	60.50	0.36	0.44	-	-	-	-	-
<i>Crossia virginiana</i>	0.46	0.42	0.51	0.76	0.92	94.00	84.60	103.40	0.61	0.75	?	?	?	?	?
<i>Brabantophyton runcariense</i>	0.20	0.18	0.23	0.33	0.41	111.00	99.90	122.10	0.72	0.88	147.00	132.30	279.30	0.47	1.00
<i>Cairoa lamanekii</i>	0.18	0.17	0.20	0.30	0.37	50.00	45.00	55.00	0.32	0.40	?	?	?	?	?
<i>Rellimia thomsonii</i>	0.11	0.10	0.12	0.18	0.22	67.92	61.13	74.71	0.44	0.54	105.00	94.50	199.50	0.34	0.71
<i>Reimannia aldenense</i>	0.11	0.10	0.12	0.18	0.22	95.00	85.50	104.50	0.62	0.75	-	-	-	-	-
<i>Tetraxylopteris schmidtii</i>	0.12	0.10	0.13	0.19	0.23	60.00	54.00	66.00	0.39	0.48	113.00	101.70	214.70	0.36	0.77
<i>Aneurophyton germanicum</i>	0.23	0.20	0.25	0.37	0.45	56.00	50.40	61.60	0.36	0.44	52.00	46.80	98.80	0.17	0.35
<i>Proteokalon petryi</i>	0.11	0.10	0.12	0.18	0.21	56.00	50.40	61.60	0.36	0.44	55.00	49.50	104.50	0.18	0.37
<i>Triloboxylon ashlandicum</i>	0.09	0.08	0.09	0.14	0.17	90.00	81.00	99.00	0.58	0.71	60.00	54.00	114.00	0.19	0.41
<i>Triloboxylon arnoldii</i>	0.16	0.14	0.17	0.26	0.32	65.00	58.50	71.50	0.42	0.52	78.00	70.20	148.20	0.25	0.53
<i>Actinoxylon banksii</i>	0.28	0.25	0.31	0.46	0.56	?	?	?	?	?	?	?	?	?	?
Gensel (1984) euphyllophyte	0.13	0.12	0.15	0.22	0.26	?	?	?	?	?	-	-	-	-	-
<i>Gothanophyton zimmermanni</i>	0.06	0.05	0.06	0.09	0.11	?	?	?	?	?	-	-	-	-	-
<i>Elkinsia polymorpha</i>	0.21	0.19	0.23	0.34	0.42	126.00	113.40	138.60	0.82	1.00	88.00	79.20	167.20	0.28	0.60
<i>Tetrastichia bupatides</i>	0.15	0.14	0.17	0.25	0.30	70.00	63.00	77.00	0.45	0.56	35.00	31.50	66.50	0.11	0.24
<i>Tristichia tripos</i>	0.41	0.37	0.45	0.67	0.82	102.00	91.80	112.20	0.66	0.81	97.00	87.30	184.30	0.31	0.66
<i>Tristichia ovensi</i>	0.14	0.13	0.16	0.23	0.29	50.00	45.00	55.00	0.32	0.40	65.00	58.50	123.50	0.21	0.44
<i>Tristichia longii</i>	0.27	0.24	0.30	0.44	0.54	90.00	81.00	99.00	0.58	0.71	85.00	76.50	161.50	0.27	0.58
<i>Laceyia hibernica</i>	0.35	0.32	0.39	0.57	0.70	96.00	86.40	105.60	0.62	0.76	53.00	47.70	100.70	0.17	0.36
<i>Yiduxylon trilobum</i>	?	?	?	?	?	85.00	76.50	93.50	0.55	0.67	75.00	67.50	142.50	0.24	0.51
<i>Calathopteris heterophylla</i>	?	?	?	?	?	70.00	63.00	77.00	0.45	0.56	60.00	54.00	114.00	0.19	0.41
<i>Langoxylon asterochlaenoideum</i>	0.30	0.27	0.33	0.49	0.60	100.00	90.00	110.00	0.65	0.79	?	?	?	?	?
<i>Triradioxylon primaevum</i>	?	?	?	?	?	50.00	45.00	55.00	0.32	0.40	45.00	40.50	85.50	0.15	0.31

Appendix C (continued)

Table 1 Continuous character scoring 3

Character	6. Width ratio at radial to bilateral domains transition (R:B diameter)					7. Max tracheid diameter in bilateral domain (μm)					8. Max diameter of recurring appendages with terete xylem (mm)				
	measure	min	max	stand min	stand max	measure	min	max	stand min	stand max	measure	min	max	stand min	stand max
<i>Psilophyton dawsonii</i>	-	-	-	-	-	-	-	-	-	-	-	-	-	-	-
<i>Stenokoleos simplex</i>	?	?	?	?	?	277.00	249.30	304.70	0.82	1.00	-	-	-	-	-
<i>Stenokoleos bifidus</i>	1.35	1.22	1.49	0.03	0.03	?	?	?	?	?	-	-	-	-	-
<i>Stenokoleos holmesii</i>	?	?	?	?	?	41.60	37.44	45.76	0.12	0.15	-	-	-	-	-
<i>Stenokoleos setchelli</i>	1.00	0.90	1.10	0.02	0.03	172.40	155.16	189.64	0.51	0.62	-	-	-	-	-
<i>Crossia virginiana</i>	?	?	?	?	?	37.50	33.75	41.25	0.11	0.14	-	-	-	-	-
<i>Brabantophyton runcariense</i>	39.17	35.25	43.09	0.82	1.00	17.64	15.88	19.40	0.05	0.06	-	-	-	-	-
<i>Cairoa lamanekii</i>	-	-	-	-	-	-	-	-	-	-	?	?	?	?	?
<i>Rellimia thomsonii</i>	-	-	-	-	-	-	-	-	-	-	?	?	?	?	?
<i>Reimannia aldenense</i>	-	-	-	-	-	-	-	-	-	-	?	?	?	?	?
<i>Tetraxylopteris schmidtii</i>	-	-	-	-	-	-	-	-	-	-	0.90	0.81	0.99	0.04	0.05
<i>Aneurophyton germanicum</i>	-	-	-	-	-	-	-	-	-	-	1.20	1.08	1.32	0.06	0.07
<i>Proteokalon petryi</i>	-	-	-	-	-	-	-	-	-	-	2.00	1.80	2.20	0.10	0.12
<i>Triloboxyton ashlandicum</i>	-	-	-	-	-	-	-	-	-	-	1.00	0.90	1.10	0.05	0.06
<i>Triloboxyton arnoldii</i>	1.60	1.44	1.76	0.03	0.04	27.27	24.54	30.00	0.08	0.10	?	?	?	?	?
<i>Actinoxylon banksii</i>	?	?	?	?	?	?	?	?	?	?	2.50	2.25	2.75	0.12	0.15
Gensel (1984) euphyllophyte	?	?	?	?	?	18.18	16.36	20.00	0.05	0.07	?	?	?	?	?
<i>Gothanophyton zimmermanni</i>	1.33	1.20	1.47	0.03	0.03	?	?	?	?	?	-	-	-	-	-
<i>Elkinsia polymorpha</i>	0.85	0.76	0.93	0.02	0.02	50.00	45.00	55.00	0.15	0.18	-	-	-	-	-
<i>Tetrastichia bupatides</i>	?	?	?	?	?	28.57	25.71	31.43	0.08	0.10	-	-	-	-	-
<i>Tristichia tripus</i>	?	?	?	?	?	25.00	22.50	27.50	0.07	0.09	-	-	-	-	-
<i>Tristichia ovensi</i>	0.81	0.73	0.89	0.02	0.02	38.46	34.61	42.31	0.11	0.14	-	-	-	-	-
<i>Tristichia longii</i>	1.13	1.02	1.24	0.02	0.03	48.88	43.99	53.77	0.14	0.18	-	-	-	-	-
<i>Laceyia hibernica</i>	?	?	?	?	?	?	?	?	?	?	-	-	-	-	-
<i>Yiduxylon trilobum</i>	?	?	?	?	?	43.75	39.38	48.13	0.13	0.16	-	-	-	-	-
<i>Calathopteris heterophylla</i>	4.44	4.00	4.89	0.09	0.11	50.00	45.00	55.00	0.15	0.18	-	-	-	-	-
<i>Langoxylon asterochlaenoideum</i>	?	?	?	?	?	33.33	30.00	36.66	0.10	0.12	-	-	-	-	-
<i>Triradioxylon primaevum</i>	0.94	0.85	1.04	0.02	0.02	50.00	45.00	55.00	0.15	0.18	-	-	-	-	-

Appendix C (continued).

Table 1 Continuous character scoring 4

Taxon	Source
<i>Psilophyton dawsonii</i>	Hartman and Banks 1980; Fig. 1
<i>Stenokoleos simplex</i>	Hoskins and Cross 1951; Beck 1960, Fig. 1
<i>Stenokoleos bifidus</i>	Beck 1960, Fig. 8
<i>Stenokoleos holmesii</i>	Matten and Banks 1969, Fig. 5, 12
<i>Stenokoleos setchelli</i>	Matten 1992, Plate 1, Fig. 1
<i>Crossia virginiana</i>	Beck and Stein 1993, Plate 1, Fig. 1, 2
<i>Brabantophyton runcariense</i>	Momont et al. 2016b, Plate 1, Fig. 1; Plate 3, Fig. 3; Momont et al. 2016a
<i>Cairoa lamanekii</i>	Matten 1973, Fig. 14
<i>Rellimia thomsonii</i>	Bonamo 1977; Dannenhoffer et al. 2007, Fig. 3,B
<i>Reimannia aldenense</i>	Stein 1982, Plate 60 Fig. 1
<i>Tetraxylopteris schmidtii</i>	Beck 1957, Fig. 14; Scheckler and Banks 1971a
<i>Aneurophyton germanicum</i>	Serlin and Banks 1978, Plate 40, Fig. 22; Schweitzer and Matten 1982
<i>Proteokalon petryi</i>	Scheckler and Banks 1971a, Fig. 7; Scheckler and Banks 1971b; Scheckler 1976
<i>Triloboxylon ashlandicum</i>	Matten and Banks 1966; Scheckler and Banks 1971a; Momont 2015, Fig 13.7
<i>Triloboxylon arnoldii</i>	Stein and Banks 1983, Fig. 14, 37
<i>Actinoxylon banksii</i>	Matten 1968
Gensel (1984) euphylllophyte	Gensel 1984, Fig. 1c, g
<i>Gothanophyton zimmermanni</i>	Remy and Hass 1986, Plate 12, Fig. 1; Scheckler et al. 2006; Momont et al. 2016b
<i>Elkinsia polymorpha</i>	Serbet and Rothwell 1992, Fig. 4, 12
<i>Tetrastichia bupatides</i>	Dunn and Rothwell 2012, Fig. 2A, 5E
<i>Tristichia tripos</i>	Galtier and Meyer-Berthaud 1996, Plate 1, Fig.2, 4
<i>Tristichia ovensi</i>	Long 1961, Plate 1, Fig. 4, 7; Galtier and Meyer-Berthaud 1996
<i>Tristichia longii</i>	Galtier 1977, Plate 1, Fig. 2, 3; Galtier and Meyer-Berthaud 1996
<i>Laceya hibernica</i>	May and Matten 1983, Fig. 4; Klavins and Matten 1996
<i>Yiduxylon trilobum</i>	Wang and Liu 2015, Fig. 2a, d
<i>Calathopteris heterophylla</i>	Long 1976, Plate 1, Fig. 2, 7
<i>Langoxylon asterochlaenoideum</i>	Scheckler et al. 2006, Plate 1, Fig. 2; Plate 2, Fig. 5
<i>Triradioxylon primaevum</i>	Barnard and Long 1974, Plate 1, Fig. 3

Appendix D

Table 2 Discrete character scoring 1

Character	9	10	11	12	13	14	15	16	17	18	19	20	21	22	23	24	25	26	27	28
<i>Psilophyton dawsonii</i>	0	0	0	0	-	0	-	-	1	-	-	0	0	-	0	0	-	0	-	-
<i>Stenokoleos simplex</i>	?	1	1	1	4	1	4	0	1	1	1	0	1	0	0	1	?	0	-	-
<i>Stenokoleos bifidus</i>	?	1	1	1	?	1	?	0	1	0	1	0	1	0	0	1	?	0	-	-
<i>Stenokoleos holmesii</i>	?	1	1	1	3	1	3	0	1	0	1	1	0	0	0	1	?	0	-	-
<i>Stenokoleos setchelli</i>	?	?	1	?	4	1	4	0	1	1	1	0	1	0	0	?	?	0	-	-
<i>Crossia virginiana</i>	?	1	?	?	?	1	3	?	1	1	1	0	1	0	0	1	?	1	?	1
<i>Brabantophyton runcariense</i>	?	1	1	1	3	1	3	1	1	1	1	0	1	0	0	1	?	1	1	1
<i>Cairoa lamanekii</i>	?	0	3	1	3	1	3/4	0	1	1	1	0	0	0	0	1	?	1	?	-
<i>Rellimia thomsonii</i>	0	0	1	1	3	1	3	0	1	1	1	0	0	1	0	1	0	1	1	1
<i>Reimannia aldenense</i>	?	0	1	1/2	3	1	3	0	1	0	1	1	0	0	0	1	?	0	-	-
<i>Tetraxylopteris schmidtii</i>	0	0	2	2	4	1	4	0	1	1	1	0	0	0	1	1	?	1	1	1
<i>Aneurophyton germanicum</i>	0	0	1	1	?	1	3	0	1	0	1	0	0	0	0	1	0	1	1	1
<i>Proteokalon petryi</i>	?	0	2	2	4	1	3/4	0	1	1	1	1	0	0	1	1	?	1	1	1
<i>Triloboxyton ashlandicum</i>	?	0	1	1	3	1	3	0	1	1	1	0	0	1	0	1	?	1	1	1
<i>Triloboxyton arnoldii</i>	?	1	1	1	3	1	3	0	1	1	1	0	0	0	0	1	?	1	1	1
<i>Actinoxylon banksii</i>	?	1	1	1	6	1	6	0	?	1	-	0	0	0	0	1	?	1	1	-
Gensel (1984) euphyllophyte	?	1	1	1	?	1	3	0	1	1	1	1	0	2	0	1	?	0	-	-
<i>Gothanophyton zimmermanni</i>	?	1	1	1	?	1	4/5/6	0	1	1	1	0	0	0	0	0	?	0	-	-
<i>Elkinsia polymorpha</i>	1	1	1	1	3	1	3	0	1	1	1	0	1	0	0	?	?	1	1	1
<i>Tetrastichia bupatides</i>	?	1	1	1	3/5	1	3/4/5/6	0	0	1	0	0	1	0	0	1	0/1	1	?	1
<i>Tristichia tripos</i>	?	1	1	1	3	1	3	0	1	1	1	0	0	0	0	1	?	1	?	1
<i>Tristichia ovensi</i>	?	1	1	1	3	1	3	0	1	0	1	0	0	0	0	1	0	1	1	1
<i>Tristichia longii</i>	?	1	1	1	3	1	3	0	1	0	0	0	0	0	0	1	?	1	1	1
<i>Laceya hibernica</i>	?	1	1	1	3	1	3	0	0	0	0	0	0	0	0	?	?	1	1	1
<i>Yiduxylon trilobum</i>	?	1	1	1	3	1	3	0	?	0	?	0	0	0	0	?	?	1	1	1
<i>Calathopteris heterophylla</i>	?	1	1	1	5	1	5	0	1	?	1	0	1	0	1	1	?	1	1	1
<i>Langoxylon asterochlaenoideum</i>	?	1	1	1	?	1	9	0	0	1	0	0	1	0	1	1	0	0	-	-
<i>Triradioxylon primaevum</i>	?	1	1	1	3	1	3	0	1	0	1	0	0	0	0	1	?	1	1	1

Appendix D (continued).

Table 2 Discrete character scoring 2

Character	29	30	31	32	33	34	35	36	37	38	39	40	41	42	43	44	45	46	47	48
<i>Psilophyton dawsonii</i>	0	0	0	1	1	0	0	0	0	-	-	-	-	-	-	-	-	-	-	-
<i>Stenokoleos simplex</i>	0	0	0	1	1	0	?	1	0	-	-	-	1	1	0	1	3	-	1	1
<i>Stenokoleos bifidus</i>	0	0	0	?	?	0	?	1	0	-	-	-	1	1	0	1	3	-	?	?
<i>Stenokoleos holmesii</i>	-	-	1	0	0	0	?	1	0	-	-	-	1	1	0	?	3	-	0	-
<i>Stenokoleos setchelli</i>	0	0	0	0	0	0	?	1	0	-	-	-	?	?	?	?	?	-	?	?
<i>Crossia virginiana</i>	0	1	0	1	1	0	?	1	0	-	-	-	?	?	-	1	?	-	?	?
<i>Brabantophyton runcariense</i>	0	0	0	1	1	0	?	0	0	-	-	-	1	1	0	1	3	-	?	?
<i>Cairoa lamanekii</i>	0	0	0	1	1	0	0	0	1	2	0	?	-	0	-	-	-	-	-	-
<i>Rellimia thomsonii</i>	0	0	0	0	0	0	0	0	1	1	0	0	-	0	-	-	-	-	-	-
<i>Reimannia aldenense</i>	0	0	0	1	1	0	1	0	?	-	-	-	-	0	-	-	-	-	-	-
<i>Tetraxylopteris schmidtii</i>	0	1	0	1	2	0	0	0	1	2	0	0	-	0	-	-	-	-	-	-
<i>Aneurophyton germanicum</i>	0	0	0	0	1	0	0	0	1	1	0	0	-	0	-	-	-	-	-	-
<i>Proteokalon petryi</i>	0	0	0	1	1	0	0	1	1	1	0	1	-	0	-	-	-	-	-	-
<i>Triloboxylon ashlandicum</i>	0	0	0	1	1	0	1	0	1	1	0	1	-	0	-	-	-	-	-	-
<i>Triloboxylon arnoldii</i>	1	0	0	1	1	0	?	0	0	-	-	-	1	1	0	1	?	?	?	?
<i>Actinoxylon banksii</i>	0	0	0	1	1	0	0	0	0	-	-	-	1	0	1	-	-	-	-	-
Gensel (1984) euphyllophyte	0	0	0	1	1	0	0	0	0	0	0/1	0	-	0	-	-	?	-	?	?
<i>Gothanophyton zimmermanni</i>	?	?	0	?	1	0	?	0	0	-	-	-	1	1	0	0	3	-	?	?
<i>Elkinsia polymorpha</i>	1	0	1	1	1	0	?	0	0	-	-	-	0	0/1	0/1	1	1	2	1	1
<i>Tetrastichia bupatides</i>	1	0	1	1/2	?	0	?	1	0	-	-	-	0	0	0	1	1/2/3	2	1	1
<i>Tristichia tripos</i>	1	0	0	1	1	0	?	1	0	-	-	-	0	0	0	1	1	2	?	-
<i>Tristichia ovensi</i>	1	0	1	1	1	0	?	1	0	-	-	-	0	0	0	1	1	2	1	1
<i>Tristichia longii</i>	1	0	1	1	1	0	?	1	0	-	-	-	1	1	0	1	1	2	?	?
<i>Laceya hibernica</i>	1	0	1	1	1	0	?	1	0	-	-	-	0	0	0	1	1	2	1	1
<i>Yiduxylon trilobum</i>	0	0	0	1	1	0	?	0	0	-	-	-	0	1	1	1	1	2	?	?
<i>Calathopteris heterophylla</i>	1	0	1	1	1	0	?	1	0	-	-	-	0	0	0	1	1	2	1	1
<i>Langoxylon asterochlaenoideum</i>	0	0	0	1	1	0	?	0	0	-	-	-	0	0	0	0	1	2	?	?
<i>Triradioxylon primaevum</i>	1	0	1	1	1	0	?	0	0	-	-	-	0	0	0	1	1	2	1	1

Appendix E

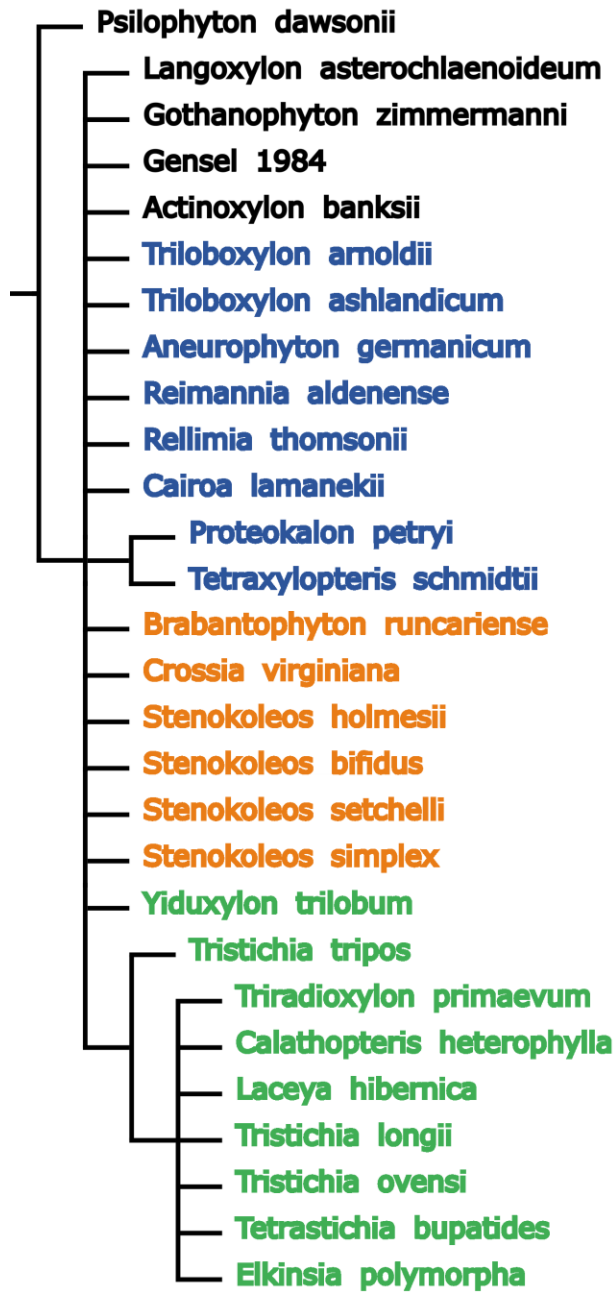


Figure 2 Strict consensus tree of 19 MP trees of 84 steps (CI = 0.548, RI = 0.683) resulting from Analysis 1, using only discrete characters. Colors indicate traditional taxonomic placement: aneurophytes and putative aneurophytes (blue), Stenokoleales (orange), and seed plants and putative seed plants (green).

Appendix F

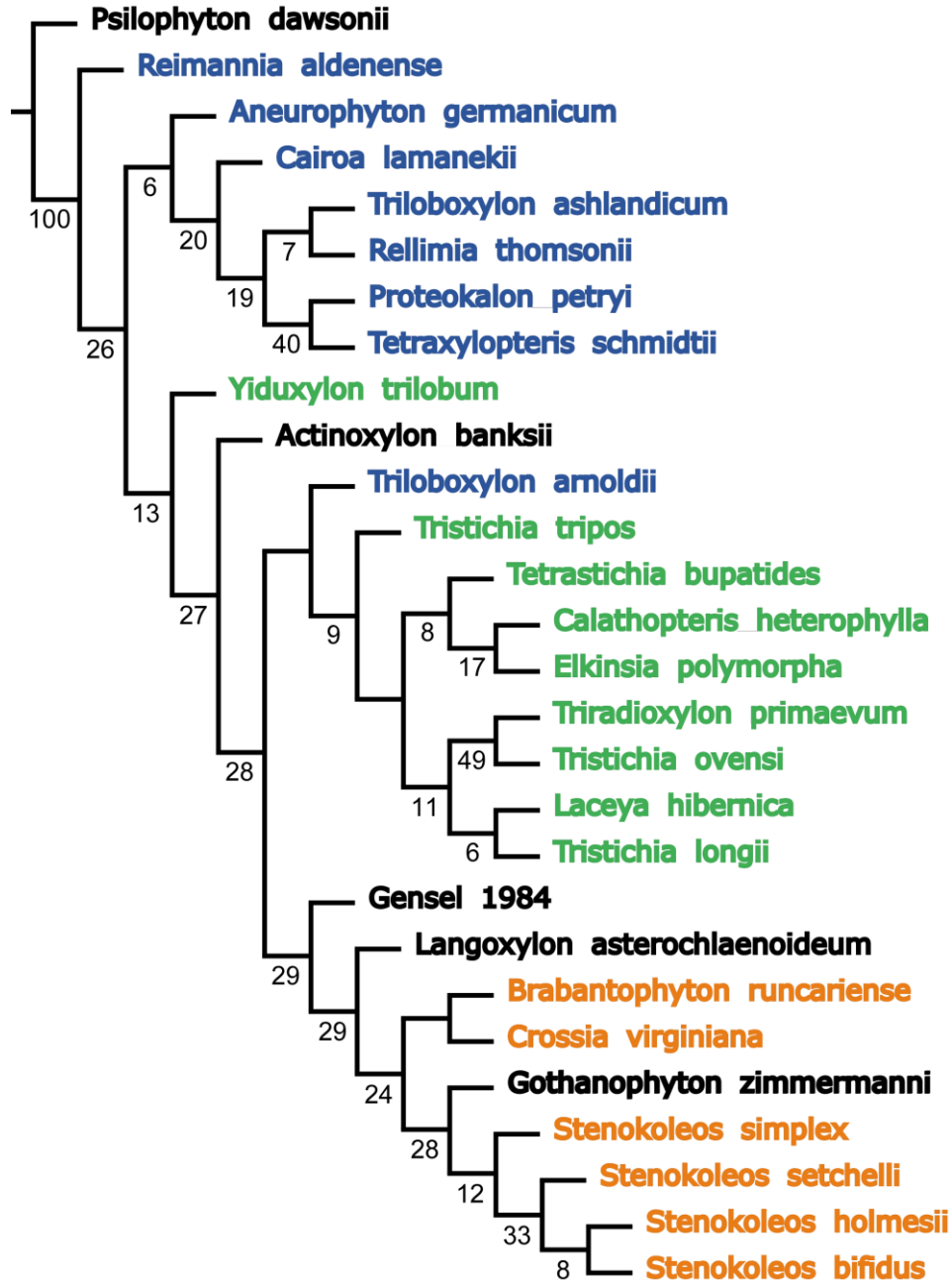


Figure 1 Single MP tree of 96.33 steps (CI = 0.528, RI = 0.656) resulting from Analysis 2, using discrete and continuous characters; numbers on branches represent bootstrap support values >5. Colors indicate traditional taxonomic placement: aneurophytes and putative aneurophytes (blue), Stenokoleales (orange), and seed plants and putative seed plants (green).

Appendix G

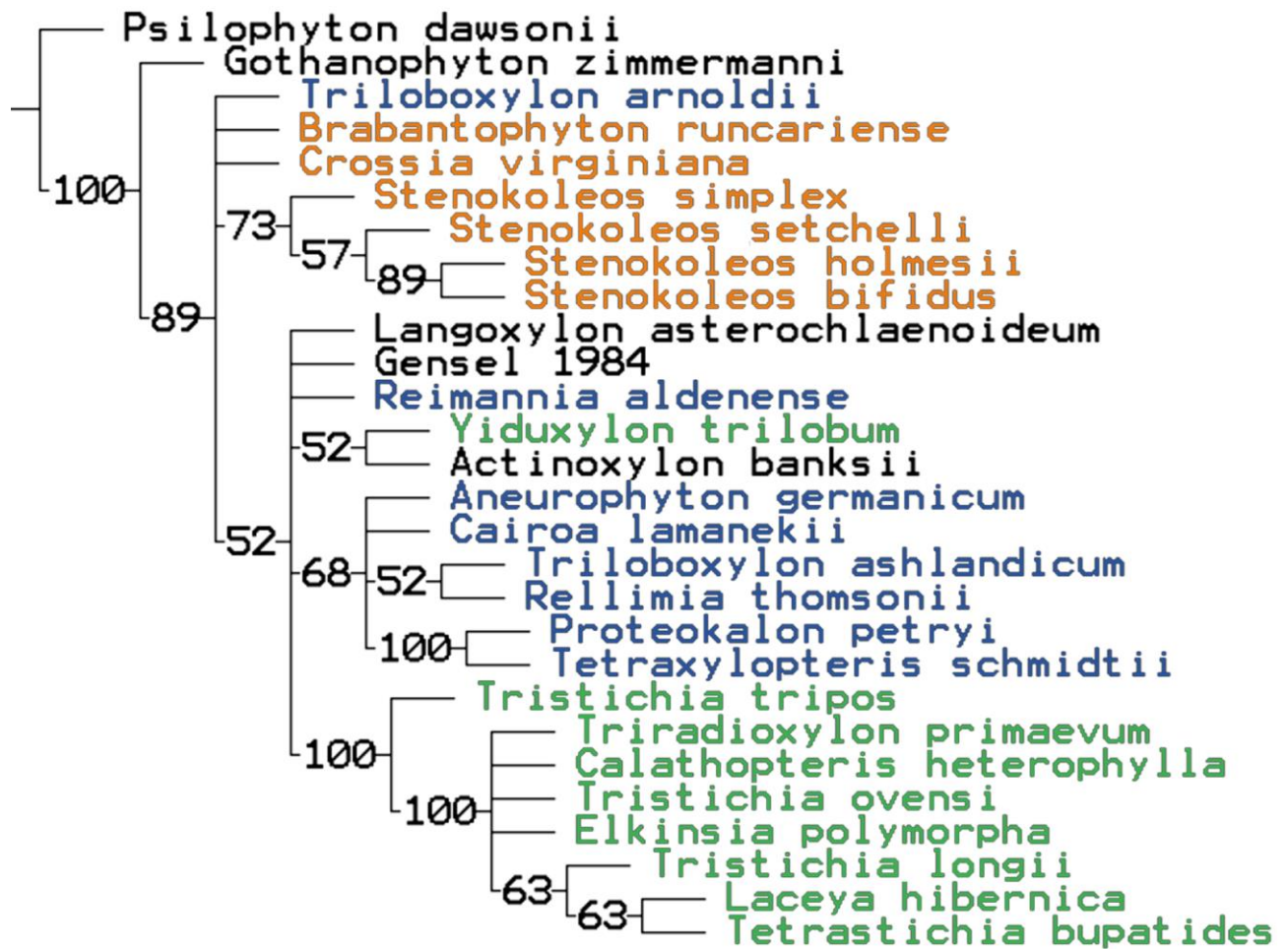


Figure 1 Majority rule consensus tree resulting from Analysis 1, using only discrete characters. Colors indicate traditional taxonomic placement: aneurophytes and putative aneurophytes (blue), Stenokoleales (orange), and seed plants and putative seed plants (green).

2. CHAPTER 2: AN EMSIAN RADIATOPSID UPDATES EARLY EUPHYLLOPHYTE PHYLOGENY POINTING TO EARLY DEVONIAN EXPLORATION OF STRUCTURAL COMPLEXITY BY MULTIPLE BASAL LINEAGES

2.1. Introduction

The Devonian explosion of land plant diversity saw the rise of all major vascular plant groups, which led from early beginnings during the last part of the Silurian to the emergence of seed plants in the Late Devonian. Within this interval, the Devonian plant fossil record shows a striking discrepancy between the Early Devonian, where we see plants with rather simple morphology and anatomy (Gensel, 2008), and later times of the Devonian, where we see lineages that show greater structural complexity (Scheckler & Banks, 1971; Beck, 1976; Scheckler, 1976; Stein, 1982; Galtier, 1988).

Among euphyllophytes, a plexus of actinostelic plants with deep-ribbed mesarch primary xylem, centered primarily around the Middle Devonian, straddles the transition between *Psilophyton*-like early euphyllophytes and the traditionally recognized euphyllophyte lineages of the Late Devonian – Early Carboniferous. Some of these plants have been assigned, with different degrees of confidence, to the spermatophytes (seed plants), progymnosperms, or Stenokoleales, while the taxonomic affinities of others have remained unresolved. Nevertheless, given their stratigraphic position and morphologies, these plants represent our only direct way to glean snapshots that document important steps of several major evolutionary processes, such as the origin of seed plants and the establishment of structurally complex sporophyte organization

in different euphyllophyte lineages. Therefore, resolution of relationships between plants in this plexus of actinostelic euphyllophytes, on one hand, and the older as well as younger euphyllophytes, on the other hand, is central to understanding these major aspects of plant evolution. However, up until recently these relationships had not been addressed in a formal phylogenetic framework.

In a recent phylogenetic study (Toledo *et al.*, 2018), we addressed the relationships between actinostelic euphyllophytes traditionally associated with discussions of seed plant origins. In that study we showed that whereas a close relationship between seed plants and Stenokoleales, to the exclusion of progymnosperms, received strongest support, tree stability was low and an alternate relationship, wherein seed plants and progymnosperms are more closely related, to the exclusion of Stenokoleales, received only marginally less support. This level of instability precludes resolution of relationships and maintains a blurry mist over the origins of euphyllophyte structural complexity and of seed plants.

Here we describe a new anatomically-preserved actinostelic radiatopsid from the Early Devonian. This new Emsian euphyllophyte is among the oldest fossils characterized by complex structure otherwise typical of Middle and Late Devonian plants, as reflected by its deeply ribbed stele, paired vascular bundles of appendage traces, and high histological differentiation. Inclusion of this new plant in a phylogenetic treatment of Devonian actinostelic euphyllophytes places it as the earliest-diverging member of this clade and stabilizes tree topology, pointing to a lignophyte clade that includes aneurophytes and seed plants, with stenokolealeans as part of a grade paraphyletic to the lignophytes. The set of relationships recovered indicates that structural complexity originated in euphyllophytes during the Early Devonian and suggests that by the end

of the Pragian ca. 408 million years ago, several euphyllophyte lineages were independently exploring structural complexity.

2.2. Materials and Methods

2.2.1. Fossil material

A total of 11 axes are preserved by cellular permineralization with calcium carbonate in four cobbles collected by Dr. Francis M. Hueber (Smithsonian Institution – NMNH) in 1965 from exposures of the Battery Point Formation on the south shore of Gaspé Bay, in the vicinity of Douglstown, Québec, Canada. The fossils, part of an allochthonous assemblage, are late Emsian in age, ca. 402–394 Ma old (see Hoffman & Tomescu, 2013). The sediments hosting the fossils were deposited in braided fluvial to costal environments (Cant & Walker, 1976; Griffing *et al.*, 2000).

Serial anatomical sections were obtained from fossil specimens using the cellulose acetate peel technique (Joy *et al.*, 1956). Slides for bright-field microscopy were mounted with Eukitt (O. Kindler, Freiburg, Germany). Images were captured using a Nikon Coolpix 8800VR digital camera mounted on a Nikon E400 compound microscope and an Olympus DP73 digital camera mounted on an Olympus SZX16 microscope. Material for scanning electron microscopy was obtained from cellulose acetate peels using the method detailed in Matsunaga *et al.* (2013). SEM images were generated using a FEI Quanta 250 (Hillsboro, Oregon, USA). Images were processed using Adobe Photoshop (San Jose, California, USA). All cobble slabs, acetate peels and slides are stored in the U.S. National Museum of Natural History – Smithsonian Institution under numbers USNM 557783, 557820, 557839, 557840.

2.2.2. Phylogenetic analyses

Kenricrana was added to the morphological matrix developed by Toledo *et al.* (2018), with the following scorings for characters 0 to 48:

0.32-0.39; 0.21-0.26; 0.75-0.92; 0.13-0.16; 0.62-0.76; 0.29-0.61; 0.04-0.05; 0.09-0.11; ?; 1; 1; 2; 4; 1; 4; 0; 1; 1; 1; ?; 0; 1; 0; 0; -; 1; 0; 0; 0; 1; 0; 1; 1; 1; ?; 0; 1; 0; 0; -; 1; 0; 0; 0; 1; 0; 1; 1; 1; ?; 0; 0; -; -; -; 1; 1; 0; 0; 1; 2; 1; 1

Kenricrana has 8.2% missing data. The matrix includes 29 anatomically preserved taxa (early euphyllophytes, aneurophytalean progymnosperms, Stenokoleales, and early seed plants), with *Psilophyton dawsonii* as outgroup. A few characters in the Toledo *et al.* (2018) matrix were rescored as follows: character 11 (number of anatomically distinct orders of branching in the radial organographic domain) rescored as “1” (changed from “0”) for *Psilophyton dawsonii*; character 33 (sclerenchyma in the outer cortex) rescored as “2” (changed from “1”) for *Tetraxylopteris schmidtii*; characters 37 (recurring appendages with terete xylem) and 38 (taxis of recurring appendages with terete xylem) rescored as “?” (changed from “0”) for Gensel’s (1984) plant; character 44 (adaxial-abaxial asymmetry of the vascular supply of the bilateral organographic domain) rescored as “?” (changed from “0”) for *Langoxylon asterochalaenoideum*.

Phylogenetic searches were conducted in TNT 1.5 (Goloboff & Catalano, 2016) following the same tree search parameters as Toledo *et al.* (2018). We used two character sampling regimes in two different analyses. The first tree search (Analysis 1) was run using only discrete characters. The second analysis included discrete plus continuous characters (Analysis

2). All characters were equally weighted and unordered to avoid *a priori* assumptions. The basic structure of the time calibrated tree was obtained with R software (R Core Team, 2017) utilizing the ‘timePaleoPhy’ and ‘geoscalePhylo’ functions of the *paleotree* and *strap* packages, respectively (Bapst, 2012; Bell & Lloyd, 2015).

2.3. Results

2.3.1. Systematics

Division Tracheophyta Cavalier-Smith 1998

Subdivision Euphyllophytina Kenrick et Crane 1997

Infradivision Radiatopses Kenrick et Crane 1997

Genus *Kenricrana* Toledo et Tomescu gen. nov.

Diagnosis: Plant with main axes bearing four-ranked, decussate, sub-opposite branches with dichotomous ultimate appendages. Main axes with central, deeply lobed, four ribbed protostele. Primary xylem maturation mesarch. Protoxylem with radiate architecture: protoxylem strands present at center of stele, along xylem rib midplanes, and at rib tips. Metaxylem tracheids with P-type tracheid pitting. Secondary xylem present all around primary xylem, tracheids with P-type pitting on radial and tangential walls. Inner cortex with sclereid nests forming discontinuous layer external to primary xylem. Outer cortex with alternating longitudinal bands of sclerenchyma and parenchyma. Pairs of Y-shaped bundles diverging tangentially from tips of primary xylem ribs to form traces that supply branches. Protoxylem gaps present at the two tips of T bar formed by tangential trace divergence. Primary branches with bilateral symmetry of vascular tissues. Anatomy of primary branches with same layering of tissues as main axes.

Secondary xylem absent. Discontinuous layer of sclereids surrounding the two Y-shaped bundles. Outer cortex primarily sclerenchymatous. Ultimate appendages supplied by two terete bundles and with anatomy similar to primary branches.

Etymology: *Kenricrana* is named in recognition of Paul Kenrick and Peter R. Crane's contributions to understanding of early tracheophyte phylogeny; these authors were also the first to illustrate a specimen, at the time unnamed, of *Kenricrana* (Kenrick & Crane, 1997, fig. 4.24.a).

Kenricrana bivena Toledo et Tomescu sp. nov.

Diagnosis: As for the genus with the following additions. Main axes ca. 5.8 mm in diameter, with four external ridges corresponding to primary xylem ribs, and four grooves corresponding to sclerenchyma strands internal to the outer cortex, between the xylem ribs. Successive decussate pairs of branches spaced at >2 cm. Primary xylem ribs ca 4 mm long and 500 μm wide, with 3-4 protoxylem strands along midplane. Metaxylem tracheids up to ca. 95 μm in diameter, consistently smaller tracheids forming discontinuous narrow bands between protoxylem strands. P-type tracheid pitting with robust secondary wall thickening exhibiting coarse spongy structure. Spaces between scalariform thickenings ca. 24 x 10 μm , covered by perforated membrane with pores 2.0-2.5 μm in diameter arranged in one to two rows. Secondary xylem tracheids with irregular shape and variable size, rectangular outline, up to 90 μm in cross section. Inner cortex broad, parenchymatous, with layer of sclereid nests up to five cells thick, ca. 100 μm away from primary xylem; sclereids 32-63 μm in diameter and > 900 μm long. Longitudinal strands of sclerenchyma in inner cortex areas between primary xylem ribs;

sclerenchyma in the strands 30-85 μm in diameter and >800 μm long. Outer cortex is ca. 350 μm thick, similar to *Sparganium*-type, with sclerenchyma 140-540 μm in diameter. Epidermis with rectangular cells 15-56 μm in size and stout capitate glandular trichomes ca. 230 μm long and expanded apex ca. 400 μm broad. Cells in trichome base elongated, storage cells in apical area have circular, 12-36 μm in diameter. Primary branches with elliptical outline, flattened in adaxial-abaxial direction, ca. 1.7-2.3 mm wide, supplied by trace consisting of small Y-shaped bundles. Protoxylem of bundles Y-shaped, metaxylem tracheids ca. 30.0 μm in diameter. Outer cortex ca. 190 μm thick, sclerenchymatous. Epidermis with glandular trichomes. Ultimate appendages, branch dichotomously at least twice.

Etymology: The specific epithet *bivena* (Latin *bi-* = two; *vena* = vein) refers to the two vascular bundles that form traces to the primary branches.

Holotype: Main axis in slab 557820-5 (Fig. 1)

Paratypes: Main axes in slabs 557783-1 (Atop through Jtop), 557839-1 (Atop through Btop), 557839-2b (Atop through Bbot), 557839-1 (Dbot) (Supporting Information Fig. S2 a-c), and primary branches in slabs 557820-1 (Abot through Btop), 557839-1 (Ctop through Dbot), 557839-1 (Dbot through Dtop), 557783-1 (Ctop through Dtop) (Supporting Information Fig. S1 b-c).

Locality and horizon: South shore of Gaspé Bay, in the vicinity of Douglstown, Quebec, Canada; Battery Point Formation, mid- to late Emsian, ca. 402–394 million years ago.

Other specimens: The unnamed specimen illustrated by Kenrick & Crane (1997, fig. 4.24.a, p. 116) from the Devonian of Gaspé (P. Kenrick, pers. comm., 05.13.2015) is a *Kenricrana bivena* axis.

Description: *Kenricrana bivena* is based on 11 specimens (six main axes and five primary branches). The longest main axis measures 12.4 cm (Supporting Information Fig. S1a) and the longest primary branch is 1.6 cm long; all specimens are fragmentary, therefore these measurements represent minimum lengths. Externally, the main axes have four ridges that correspond to primary xylem ribs (Fig. 1a). The diameter of main axes is 4.62–7.61 mm. Primary branches have sub-opposite, four-ranked, decussate taxis, with successive pairs diverging at more than 2 cm apart (ca. 2.2 cm in 557839-2b; 2.9 cm and 4.4 cm in 557783-1). They are flattened in the adaxial-abaxial direction, with more-or-less elliptical outline, 0.84-1.25 x 1.75-2.21 mm in cross section (Fig. 1b, Fig. S1b, c). Ultimate appendages are alternately arranged on primary branches, spaced at ca. 5 mm, and branch dichotomously at least twice.

Main axes have a central, deeply lobed protosteles with four ribs of primary xylem. Primary phloem is found around the primary xylem (Fig. 1a, Fig. S3d, e). One specimen has a thin layer of secondary xylem around the primary xylem (Fig. 1c). Axes have a cortex with distinct layers. The thick inner cortex includes sclereid nests, which form a discontinuous layer external to the primary xylem. The rest of the inner cortex was parenchymatous. The outer cortex consists of longitudinal bands of sclerenchyma that alternate with parenchymatous areas. Four sclerenchyma clusters extend inwards from the outer cortex into the inner cortex, in the areas between the xylem ribs. The epidermis holds capitate glandular trichomes. Primary branches exhibit the same layering of tissues as the main axes (Fig. 1b, Fig. S1b, c), except for secondary xylem, which is absent in the specimens studied, and for the outer cortex which is primarily sclerenchymatous and does not always include parenchyma.

Main axes—The epidermis, discontinuously preserved, consists of cells rectangular in cross section (Fig. 1d), 15.6-56.0 μm in size (mean = 30.7 μm , n=19), and slightly elongated in longitudinal section (216.0-336.0 μm ; mean = 280.0 μm , n=3). The outer periclinal wall is often thicker in the epidermal cells, probably reflecting a cuticle layer. Capitate glandular trichomes project from the epidermis ca. 225 μm (Supporting Information Fig. S3a, b). They have a stout base and a slightly expanded apex (ca. 408 μm broad). Cells in the trichome base are elongated, 96.0-192.0 μm (mean = 132.3 μm , n=8). The storage cells in the expanded apical area have circular outline and are smaller than the epidermal cells, 12.0-36.0 μm in diameter (mean = 24.9 μm , n=19).

The outer cortex is ca. 350 μm thick and it consists of tangentially alternating areas of well-preserved sclerenchyma and areas occupied by parenchyma cells, which are less frequently preserved (Fig. 1a, e). In cross sections, the sclerenchyma cells are roughly rectangular, with wide lumen, and 144.0-540.0 μm (mean = 337.9 μm , n = 19) in diameter. The outer cortex is similar to the *Sparganum*-type cortex documented in aneurophytalean progymnosperms, stenokolealeans, and early seed plants [e.g., *Triloboxylon ashlandicum* (Scheckler & Banks, 1971), *Stenokoleos simplex* (Beck, 1960), *Elkinsia polymorpha* (Serbet & Rothwell, 1992)].

Longitudinal strands of sclerenchyma form, in cross sections, clusters that protrude from the outer cortex into the inner cortex, in the four sectors corresponding to the areas between the primary xylem ribs (Fig. 1a, f, Fig. S2a-c). The cells that form these strands are variable in cross-sectional diameter and shape [31.2 to 52.8 μm], as well as cell wall thickness. Their minimum length, as observed in oblique sections, is 801.6 μm . Scattered among the sclerenchyma, some of the cells have significantly thinner walls, suggesting that they may be parenchyma. Cells on

the innermost side of the four sclerenchyma strands resemble the sclereids that form nests in the inner cortex. They have circular outline and very thick secondary walls although their thickness varies somewhat. These cells are 37.2-84.0 μm (mean = 56.1 μm , n = 19) in diameter and at least 800 μm long.

The inner cortex is broad and consists primarily of parenchyma, which are rarely preserved. Nests of sclereids (Fig. 1a, Fig. S2a-c) form a discontinuous but consistently present layer in the vicinity of the xylem (ca. 103.5 μm away from it). The layer is up to five cells thick and follows closely the outline of the primary xylem (Fig. 2a). Cell size and wall thickness, as seen in cross section show little variation across the layer (close to average). The sclereids are longitudinally elongated and sometimes branched (Fig. S3c). They are 32.4-62.4 μm in diameter (mean = 42.4 μm , n = 19) and at least 912.0 μm long.

Phloem probably formed a layer immediately outside the xylem and bordered by the layer of sclereid nests. Phloem may have consisted of narrow cells (ca. 102.3 μm in diameter) with thin walls, as suggested by the cell wall remnants seen on the outer walls of the outermost primary xylem tracheids, where they would have been in contact with the phloem (Fig. S3d, e).

The primary xylem ribs are long (1440.0-4200.0 μm ; mean = 2213.1 μm , n = 19) and narrow (240-552 μm) in cross sections (Fig. 1a, Fig. S2a-c). Primary xylem maturation is mesarch and protoxylem strands are present in the center of the stele, along the midplane of xylem ribs (3-4 protoxylem strands along each rib), and at the tips of each rib (Fig. 1a, 2a, Fig. S3f). This corresponds to radiate protoxylem architecture (Beck & Stein, 1993). Along the midplanes of primary xylem ribs, metaxylem tracheids consistently smaller than in the rest of the xylem form discontinuous narrow bands between the protoxylem strands (Fig. S3f). Metaxylem

tracheids are up to 96.0 μm in diameter and at least 1773.5 μm long. The secondary wall thickening pattern is comparable to the *Psilophyton*-type (P-type) thickenings of basal euphyllophytes (such as *Franhueberia* and *Armoricaphyton*; Hoffman & Tomescu, 2013; Strullu-Derrien *et al.*, 2014). Secondary wall thickenings form a scalariform pattern, with spaces between the thickenings (ca. 24.3 μm wide and 10.0 μm tall) covered by a perforated membrane with pores 2.0-2.5 μm in diameter (Fig. 2d, e). The pores are usually arranged in one, sometimes two horizontal rows, and rarely in a less regular pattern. Seen in longitudinal sections, the scalariform thickenings have a coarse spongy structure and exhibit geometry similar to that of bordered pits (Fig. 2f, Supporting Information Fig. S4a, b).

Gaps (open areas) are present at the location of protoxylem strands occupying the two tips of the T bar formed when traces to branches diverge tangentially from the tips of primary xylem ribs (Fig. 3d). These gaps are not always observed, in these locations, in all primary xylem ribs. While this is in part due to taphonomic distortion of the tips of xylem ribs in many locations, cases of good preservation demonstrate that the gaps have limited longitudinal extent. This characteristic and the lack of both parenchyma cells and of remnants of elongated and torn protoxylem tracheids, suggest that the gaps do not correspond to peripheral loops (*sensu* Read, 1938), or to rhexigenous lacunae, such as those seen in the carinal canals of *Equisetum*. Additionally, no other tissues of the main axes contain big aerenchymatous areas that would be consistent with rapid elongation during development. Based on their features, these protoxylem gaps are best interpreted as having a lysigenous nature.

Secondary xylem is known only from an axis fragment consisting of one xylem rib (Fig. 1c). In this specimen, the primary xylem is surrounded by radially aligned tracheids with

rectangular outlines, up to 90.0 μm in cross section. These tracheids form radial files up to 5-6 cells long on both sides of the primary xylem rib. Secondary xylem tracheids are more abundant around the tip of the rib, forming a thicker layer, with radial files of up to 9-12 cells. The secondary xylem is up to 528.0 μm thick around the tip of the primary xylem rib and as thin as 96.0 μm at the most proximal end of the rib. Secondary xylem tracheids exhibit the same type of P-type pitting as the metaxylem, on both radial and tangential walls (Fig. 3b, c).

Branching anatomy—The vascular supply of primary branches departs from the tips of primary xylem ribs. In the basal-most portions of trace divergence, the tip of the primary xylem rib expands tangentially, producing a T shape. The peripheral protoxylem strand (at the rib tip) branches in a tangential plane forming two strands that supply the two tips of the T bar (Fig. 3d). In most specimens, the peripheral protoxylem strands and those of the T bar are compressed and the tracheids collapsed (Fig. 3d). Nevertheless, some helical secondary wall thickenings can be seen in longitudinal sections even in such compressed strands (Fig. 3a). The two protoxylem strands of the T bar host gaps (Fig. 3d). Distally, each of the two tips of the T bar forms two lobes in a V-shape (Fig. 3e). Higher up, the two tips of the T bar diverge from the xylem rib forming two vascular bundles (Fig. 3f). These bundles, which enter the base of the primary branch, are Y-shaped (with the base of the Ys pointing toward each other). At this level, the two bundles consist of few, small metaxylem tracheids (up to 44.4 μm in diameter and at least 720.0 μm long) that form a thin layer around the Y-shaped area of protoxylem (Fig. 2b, c). Because individual tracheids cannot be discerned in these protoxylem areas, it is possible that the protoxylem is entirely collapsed in the primary branch traces due to taphonomic factors. The layer of sclereid nests in the inner cortex of main axes follows closely all the changes in shape of

the primary xylem rip tips associated with the production of branch traces (Fig. 3e). When the paired bundles that form the primary branch trace diverge from the main axis stele, as they traverse the cortex they are surrounded by a common layer of sclereid nests very similar, positionally, to the layer found in main axes.

Primary branches—Primary branches have an elliptical overall shape in cross section and exhibit bilateral symmetry of the xylem. They have two vascular bundles similar in shape and arrangement to the paired traces that diverge from the xylem ribs of main axes. The two bundles are Y-shaped, with protoxylem represented by dark lines (Y-shaped) at the center, or sometimes preserving helical secondary wall thickenings, and surrounded by few small metaxylem tracheids (Fig. 1b, 2b, c, Supporting Information Fig. S1b, c) up to 30.0 μm in diameter. Phloem remnants are recognized locally and are similar to those of main axes (Fig. 2b, c). The two bundles are surrounded by a common layer of sclereid nests of the same nature as those present in the main axes. Outside the sclereid nest layer, the inner cortex is partially preserved and consists of parenchyma. The outer cortex, ca. 190 μm thick, is primarily sclerenchymatous, consisting of cells with thick secondary walls. Sometimes it can exhibit the same *Sparganium*-type anatomy as the outer cortex of main axes, albeit less marked. The epidermis is comparable to that of main axes, including presence of glandular trichomes.

Primary branches bear small sized appendages that are arranged alternately or sub-oppositely in a horizontal plane and that are supplied by two terete vascular bundles (Fig. S3g). Incomplete preservation has precluded detailed observations on the departure of the appendage vasculature from the primary xylem of the branches. We hypothesize that the two vascular bundles in the appendages originate from the two tips of the Y-shaped bundle. The overall

anatomy of tissues in these appendages is similar to that of primary branches and the main axes, with a parenchymatous inner cortex (including sclereid groups) and sclerenchymatous outer cortex.

Remarks on secondary growth—Although it is an isolated fragment, the specimen consisting of a xylem rib portion with anatomy reminiscent of secondary xylem (Fig. 1c) belongs to *Kenricrana* because it shares with the intact axes of the latter the same type of metaxylem tracheid pitting, shape and size, and the same protoxylem distribution (forming black lines, in the same pattern, because of compression). Furthermore, only one other plant known to date from the Gaspé cobbles that features an actinostele with ribs of comparable size is a cladoxylopsid, which does not have P-type metaxylem tracheid pitting and has, instead, distinctive circular bordered pits.

Secondary xylem is recognized by (1) radially aligned tracheids in transverse section, (2) presence of multiplicative (anticlinal) divisions, which increase the number of radial tracheid files, and (3) xylem rays which form a radial system within the otherwise vertically oriented tracheids (Hoffman & Tomescu, 2013). The *Kenricrana* fragment does not exhibit unequivocally all the diagnostic features of secondary xylem. For instance, while some structures could represent multiplicative divisions (Fig. 3h, i), distortion of the specimen makes it difficult to demonstrate with certainty that those features are multiplicative divisions. We were also unable to identify with certainty rays, for the same reason as above. However, with radial files of tracheids only about 5-12 cells long, if this specimen shows early stages of secondary growth, uniseriate rays would have been inconspicuous even in the living plant, let alone in a specimen fossilized under harsh conditions (like those implied by the preservation of our specimen); see, for comparison, an extant conifer root with the same amount of secondary

growth (Fig. 3g), in which rays are equally inconspicuous. Likewise, multiplicative divisions would have been rare at this early stage of secondary growth (compare to Fig. 3g).

Despite the lack of unequivocal rays and multiplicative divisions, we interpret this specimen as an instance of secondary growth produced by a cambium for several reasons. First, the specimen displays marked, regular radial arrangement of tracheids at the periphery of the xylem, in stark contrast to the arrangement of tracheids that occupy a central position in the xylem (primary xylem). Second, the radially aligned tracheids have different shapes and sizes than those in the central xylem – they are predominantly rectangular, most of them are radially elongated and many are larger than the central tracheids. Third, within each radial file, tracheid size decreases toward the periphery of the xylem, in the same pattern as that observed in secondary xylem, in vicinity of the cambium, in extant seed plants.

2.3.2. Phylogenetic position of *Kenricrana*

Analysis 1 (discrete characters only) —This search resulted in 26 most parsimonious (MP) trees (tree length 90; CI = 0.50, RI = 0.62). The consensus tree (Supporting Information Fig. S5) is similar to that obtained by Toledo *et al.* (2018) using discrete characters. A basal polytomy includes *Kenricrana*, *Gothanophyton*, and a clade representing the rest of the ingroup. This clade is a massive polytomy, within which only two clades are resolved: one including *Proteokalon* + *Tertraxylopteris*, and the other, also polytomic, including seven of the nine seed plants in the analysis.

The majority rule consensus tree (Supporting Information Fig. S6) shows the same basal polytomy between *Kenricrana*, *Gothanophyton*, and a clade representing the rest of the ingroup.

Within this clade, a basal polytomy separates the stenokolealeans (*Stenokoleos*, forming a clade, *Crossia*, and *Brabantophyton*) and *Triloboxylon arnoldii* from aneurophytealean progymnosperms and seed plants, which form a clade. This topology is highly similar to that of the majority rule consensus tree obtained by Toledo *et al.* (2018) using discrete characters only, without *Kenricrana*.

Analysis 2 (discrete + continuous characters) —The search produced one MP tree (tree length 102.78; CI = 0.49, RI = 0.60) (Fig. 4). Continuous characters improved resolution substantially, while maintaining the general tree topology of the majority rule consensus tree based on discrete characters only. Overall, the ingroup consists of a paraphyletic grade basal to a lignophyte clade within which a basal divergence separates an aneurophyte clade from a seed plant clade. The paraphyletic grade features a basally-diverging *Kenricrana*, followed by *Gothanophyton*, the *Stenokoleos* clade, another stenokolealean clade (*Crossia* + *Brabantophyton*), *Langoxylon*, and Gensel's (1984) plant. Within the lignophyte clade, the seed plant clade is sister to *Triloboxylon arnoldii*, a putative aneurophyte, and the aneurophyte clade has *Actinoxylon* (putative progymnosperm) and *Yiduxylon* (putative seed plant) paraphyletic at the base.

2.4. Discussion

2.4.1. Phylogenetic relationships

The major plant groups considered in this analysis are aneurophytalean progymnosperms, stenokolealeans, and actinostelic seed plants, along with a few additional satellite taxa of uncertain affinities. The overall system of relationships we recovered features a paraphyletic grade that includes *Kenricrana*, stenokolealeans, and a few of the satellite taxa [*Gothanophyton*, *Langoxylon*, Gensel's (1984) plant], leading up to a clade within which aneurophytes and seed plants are well separated into two sister clades, with a few exceptions consisting of more contentious representatives of the two groups. The fact that the three traditional groups are recovered as phylogenetically distinct, despite the lack of reproductive characters (which are unknown for many of them) demonstrates that the vegetative morpho-anatomical characters used in traditional taxonomy of this plexus of plants bear a strong phylogenetic signal. This was also indicated by our earlier analyses (Toledo *et al.*, 2018). However, those analyses demonstrated significant instability of relationships between the three major groups, whereby either the stenokoleales or the aneurophytes were recovered as more closely related to the seed plants, with the former only marginally better supported than the latter. Here, inclusion of the new species, *Kenricrana bivena*, improved stability, tipping the balance toward a closer relationship between aneurophytes and seed plants.

Because of their lower character-to-taxon ratios and higher relative incidence of homoplasy, morphological datasets typically result in lower measures of branch support, as judged by molecular phylogenetic standards. Nevertheless, the strength of their results can be

judged qualitatively in terms of branch stability (as demonstrated by experiments with inclusion-exclusion of taxa or characters, e.g., Lantz *et al.*, 1999; Rothwell, 1999; Rothwell & Nixon, 2006). Thus, it is notable that inclusion of *Kenricrana bivena* resulted in trees that recover the same set of relationships whether continuous characters are used or not (compare Fig. 4 and Fig. S6) and that these relationships are closely similar to the relationships recovered without inclusion of *Kenricrana* when using discrete characters only (Appendix 7 of Toledo *et al.*, 2018).

This more stable set of relationships excludes the Stenokoleales from among the lignophytes, a position that we had hypothesized earlier (Toledo *et al.*, 2018). Furthermore, our results suggest that the Stenokoleales, as currently defined, are not monophyletic. Instead, taxa currently included in the group represent at least two distinct lineages: a *Stenokoleos* clade and a clade exhibiting secondary xylem (*Crossia* + *Brabantophyton*).

The taxonomic placement of taxa of more contentious affinities have been discussed extensively by Toledo *et al.* (2018). Current results warrant a few additional considerations. *Langoxylon* forms with the two stenokolealean clades a grade characterized by presence of protoxylem parenchyma, a feature lost in the sister group of *Langoxylon* and that re-appears in the *Tetrastichia-Calathopteris-Elkinsia* clade. The position of *Triloboxylon arnoldii* as sister to a seed plant clade implies either that this species is a misidentified seed plant (its reproductive structures are unknown) or that, if it is an aneurophyte, then aneurophytes form a grade, given that the remaining aneurophytes are grouped in a clade that is sister to the *T. arnoldii* + seed plants clade. However, the clade including most of the aneurophytes has at the base a grade consisting of *Actinoxylon* and *Yiduxylon*, two plants of uncertain affinities – the former a putative progymnosperm and the latter a putative seed plant. Resolution of these relationships at the base

of the aneurophyte and seed plant clades will greatly benefit from knowledge of the reproductive structures of these plants.

Kenricrana bivena is a new addition to a very short list of euphyllophytes [*Gothanophyton* + Gensel's (1984) plant] that cross the boundary of the Early Devonian providing the oldest evidence of mesarch actinosteles. *Kenricrana* shares features such as a deeply ribbed stele, paired vascular bundles in appendage traces, and outer cortex with alternating parenchyma and sclerenchyma bands, with the aneurophytalian progymnosperms, stenokolealeans, and seed plants. These similarities, along with its protoxylem architecture, place *Kenricrana* firmly among the Radiatopses [i.e. Beck & Stein's (1993) radiate protoxylem group]. However, its unique combination of characters that includes bilaterally symmetrical appendages lacking adaxial-abaxial polarity, tangential divergence of traces to laterals from the stele of the main axis, capitate glands, nests of sclereids in the inner cortex, and P-type tracheid pitting, places *Kenricrana* outside of all these three groups, in an early-diverging position, as the sister to the rest of the ingroup of actinostelic euphyllophytes. Thus, taxonomically *Kenricrana* can only be considered, for now, a basal euphyllophyte. We predict that addition of other new species from the Early Devonian to analyses like this one will lead to assembly of a better defined taxonomic framework for *Kenricrana* and similar plants. In this context, we note that the next steps should involve inclusion of archaeopteridalian progymnosperms and cladoxylopsids into these analyses.

2.4.2. Evolution of plant structure

The phylogenetic relationships supported by our data suggest that euphyllophytes with axes displaying bilateral symmetry (in their anatomy), i.e., a bilateral organographic domain, arose no later than the Pragian. This implies that the aneurophyte “habit”, characterized by the absence of a bilateral organographic domain represents a reversal in terms of the anatomy of the xylem supply of sporophyte architecture. Furthermore, adaxial-abaxial asymmetry, a feature typical of leaves and reflected in the xylem anatomy of lateral axes in our euphyllophyte dataset, is also predicted to have evolved in before the Emsian (Fig. 4) and is part of a morpho-anatomical syndrome that characterizes the stenokolealean grade, along with the presence of protoxylem parenchyma. However, in contrast to the latter character, which is reversed in the clade including lignophytes and Gensel’s (1984) plant, adaxial-abaxial asymmetry of laterals persisted in the seed plants.

Secondary growth is thought to have originated independently in multiple lineages of the euphyllophyte clade (Spicer & Groover, 2010; Boyce, 2010; Hoffman & Tomescu, 2013). In this study, potentially independent origins include the lignophyte clade, the *Crossia* + *Brabantophyton* clade, and *Kenricrana* (Fig. 4). The latter is the fourth Early Devonian plant recognized with secondary growth, along with *Armoricaphyton* (Gerrienne *et al.*, 2011; Strullu-Derrien *et al.*, 2014), *Franhueberia* (Hoffman & Tomescu, 2013), and an unnamed euphyllophyte (Gerrienne *et al.*, 2011), each of which could represent additional independent origins of secondary growth in the clade. Given these multiple occurrences of secondary growth in a diverse range of euphyllophyte lineages, several of which occupy basal positions in the clade

both phylogenetically and in terms of absolute age, the possibility of a single origin of secondary growth in euphyllophytes should be seriously considered in future studies.

For all its similarities with aneurophytes, stenokolealeans, and seed plants, *Kenricrana* is distinctly different from all these Middle- and Late Devonian groups in the pitting of its tracheids. Whereas these younger radiatopsids have bordered pits, *Kenricrana* has P-type secondary wall thickenings. P-type tracheids characterize the xylem of basal euphyllophytes with simple morphology (*Psilophyton*, *Armoricaephyton*; Kenrick & Crane, 1997; Strullu-Derrien *et al.*, 2014). Thus, this plesiomorphic type of tracheid pitting persists into the end of the Early Devonian, in plants such as *Kenricrana*, *Gothanophyton* (Remy & Hass, 1986), and an additional array of actinostelic euphyllophytes recently discovered in the Battery Point Formation (Bickner & Tomescu, unpublished). These plants exhibit features of structural complexity – ribbed steles, complex traces to laterals, histological differentiation in the inner and outer cortex. Together, these suggest that a plexus of Early Devonian euphyllophytes characterized by plesiomorphic tracheids were already making inroads into the morphospace of structural complexity explored to a fuller extent in the Middle Devonian and later times by euphyllophyte lineages that produced bordered pits. Perhaps more importantly, the topology of our phylogeny and the age constraint placed by the early Emsian age of Gensel’s (1984) plant, as well as the structural complexity exhibited by Emsian plants (Gensel’s plant, *Gothanophyton*, *Kenricrana*), suggest that by the end of the Pragian ca. 408 million years ago, several euphyllophyte lineages were independently exploring structural complexity. Aside from *Kenricrana*, *Gothanophyton*, and Gensel’s (1984) plant, these lineages included two stenokolealean stem groups, as well as the lignophyte stem.

2.5. Conclusions

We describe a new basal euphyllophyte, *Kenricrana bivena*, represented by anatomically-preserved specimens from the mid-late Emsian (402-394 Ma) of Gaspé (Canada). *Kenricrana* is a radiatopsid that shares basic anatomical features with species of three major plant groups recognized in Middle Devonian and younger rocks (Aneurophytales, Stenokoleales, and seed plants): deeply ribbed stele, paired vascular bundles in appendage traces, and outer cortex with alternating parenchyma and sclerenchyma bands. However, *Kenricrana* cannot be included in any of these groups because of its distinct combination of characters: bilaterally symmetrical appendages that lack adaxial-abaxial polarity, tangential divergence of traces to laterals from the stele of the main axis, capitate glands, nests of sclereids in the inner cortex, and P-type tracheid pitting. Discovery of *Kenricrana* and several other euphyllophytes that have yet to be fully characterized (Chu & Tomescu, 2015; Bickner *et al.*, 2017) in the Emsian rocks of Gaspé signals that continued exploration of Early Devonian strata stands to reveal additional fossil diversity that will improve our understanding of the phylogeny of basal euphyllophytes, lignophytes, and seed plants, and will illuminate the evolution of plant structural complexity.

In a phylogenetic context, addition of *Kenricrana* to a dataset that includes actinostelic euphyllophyte lineages associated with the origin of seed plants introduces stability in the relationships between these lineages. The overall pattern of relationships recovered places *Kenricrana* as sister to the rest of the ingroup, within which a paraphyletic grade of stenokolealeans and other taxa [*Gothanophyton*, *Langoxylon*, Gensel's (1984) plant] leads up to

a clade wherein a basal divergence separates a clade including seed plants from a clade including aneurophytes. Addition of cladoxylopsids and archaeopteridalean progymnosperms in future phylogenetic treatments of taxa included in the current study will improve understanding of relationships among basal euphyllophytes.

Kenricrana adds a fourth distinct occurrence of secondary growth in the Early Devonian. Together, these Early Devonian plants exhibiting secondary growth positioned close to the base of the euphyllophytes raise the question of the possibility of a single common origin of secondary growth in this clade. *Kenricrana* also adds a third species to the short list of structurally complex plants described to date from pre-Middle Devonian rocks. Along with *Gothanophyton* and Gensel's (1984) euphyllophyte, *Kenricrana* contributes to bridging the morphological gap between Emsian and older euphyllophytes of simple structure and the structurally-complex plants of the Middle and Late Devonian. These plants indicate that structural complexity originated in euphyllophytes during the Early Devonian and suggest that independent exploration of structural complexity by diverse euphyllophyte lineages was well underway by the end of the Pragian, ca. 408 million years ago.

References

- Bapst DW. 2012.** Paleotree: an R package for paleontological and phylogenetic analyses of Evolution. *Methods in Ecology and Evolution* **3**: 803–807.
- Beck CB. 1957.** *Tetraxylopteris schmidtii* gen. et sp. nov., a probable pteridosperm precursor from the Middle Devonian of New York. *American Journal of Botany* **44**: 350-367.
- Beck CB. 1960.** Studies of New Albany Shale plants. I. *Stenokoleos simplex* comb. nov. *American Journal of Botany* **47**: 115-124.
- Beck CB. 1976.** Current status of the Progymnospermopsida. *Review of Palynology and Paleobotany* **21**: 5-23.
- Beck CB, Stein WE 1993.** *Crossia virginiana* gen. et sp. nov., a new member of the Stenokoleales from the Middle Devonian of southwestern Virginia. *Palaeontographica B* **229**:115-134.
- Bell MA, Lloyd GT. 2015.** strap: an R package for plotting phylogenies against stratigraphy and assessing their stratigraphic congruence. *Palaeontology* **58**: 379–389.
- Bickner M, Toledo S, Tomescu AMF. 2017.** *New fossils from the Battery Point Formation of Gaspé (Quebec, Canada) expand the anatomical diversity of Early Devonian euphyllophytes.* [WWW document] URL <http://2017.botanyconference.org/engine/search/index.php?func=detail&aid=166>. [accessed 12.07.2017]
- Boyce CK. 2010.** The evolution of plant development in a paleontological context. *Current Opinion in Biology* **13**:102–107.
- Cant DJ, Walker RJ. 1976.** Development of a braided-fluvial facies of model for the Devonian Battery Point Sandstone, Quebec. *Canadian Journal of Earth Sciences* **13**: 102-119.
- Chu J, Tomescu AMF. 2015.** *Reappraising the flora of the Battery Point Formation (Québec) – additional diversity of Early Devonian permineralized plants.* [WWW document] URL <http://2015.botanyconference.org/engine/search/index.php?func=detail&aid=753>. [accessed 12.07.2017].
- Crane PR. 1985.** Phylogenetic relationships in seed plants. *Cladistics* **1**: 329–348.

- Dannenhoffer JM, Bonamo PM. 2003.** The wood of *Rellimia* from the Middle Devonian of New York. *International Journal of Plant Sciences* **164**: 429-441.
- Dannenhoffer JM, Stein W, Bonamo PM. 2007.** The primary body of *Rellimia thomsonii*: integrated perspective based on organically connected specimens. *International Journal of Plant Science* **168**: 491-506.
- Doyle JA, Donoghue MJ. 1986.** Seed plant phylogeny and the origin of angiosperms: An experimental cladistic approach. *The Botanical Review* **52**: 321–431.
- Galtier J, Meyer-Berthaud B. 1996.** The early seed plant *Tristichia tripos* (Unger) comb. nov. from the Lower Carboniferous of Saalfeld, Thuringia. *Review of Paleobotany and Palynology* **93**: 299-315
- Gensel PG. 1984.** A new Lower Devonian plant and the early evolution of leaves. *Nature* **309**: 785-787.
- Gensel PG. 2008.** The earliest land plants. *Annual Review of Ecology, Evolution, and Systematics* **39**:459–77.
- Gerrienne P, Meyer-Berthaud B, Lardeux H, Regnault S. 2010.** First record of *Rellimia* Leclercq & Bonamo (Aneurophytales) from Gondwana, with comments on the earliest lignophytes. In M. Vecoli, G. Clement, B. Meyer-Berthaud [eds], *The terrestrialization process: modelling complex interactions at the biosphere-geosphere interface*, 81-92. The Geological Society, London, UK.
- Goloboff PA, Catalano SA. 2016.** TNT version 1.5, including a full implementation of phylogenetic morphometrics. *Cladistics* **32**: 221-238.
- Griffing DH, Bridge JS, Hotton, C. L. 2000.** Coastal fluvial paleoenvironments and plant paleoecology of the Lower Devonian (Emsian), Gaspé Bay, Quebec, Canada. *Geological Society, London, Special Publications* **180**: 61: 84.
- Hartman CM, Banks HP. 1980.** Pitting in *Psilophyton dawsonii*, an Early Devonian trimerophyte. *American Journal of Botany* **67**: 400-412.
- Hoffman LA, Tomescu AM. 2013.** An early origin of secondary growth: *Franhueberia gerriennei* gen. et sp. nov. from the Lower Devonian of Gaspé (Quebec, Canada). *American Journal of Botany* **100**: 754-763.

- Hoskins CH, Cross AT. 1951.** The structure and classification of four plants from the New Albany Shale. *The American Midland Naturalist* **46**: 684-716.
- Joy KW, Willis AJ, Lacey WS. 1956.** A rapid cellulose peel technique in botany. *Annals of Botany* **20**: 635-637.
- Kenrick P, Crane PR. 1997.** *The origin and early diversification of land plants: a cladistics study*. Washington and London: Smithsonian Institution Press.
- Lantz TC, Rothwell GW, Stockey RA. 1999.** *Conantiopteris schuchmanii*, gen. et sp. nov., and the role of fossils in resolving the phylogeny of Cyatheaceae *s.l.* *Journal of Plant Research* **112**: 361-381.
- Matsunaga KKS, Stockey RA, Tomescu AM. 2013.** *Honegeriella complexa* gen. et sp. nov., a heteromorous lichen from the Lower Cretaceous of Vancouver Island (British Columbia, Canada). *American Journal of Botany* **100**: 450-459.
- Matten LC. 1992.** Studies on Devonian plants from New York State: *Stenokoleos holmesii* n. sp. from the Cairo Flora (Givetian) with an alternative model for lycopod seed fern evolution. *Courier Forschungs-Institut Senckenberg* **147**: 75-85.
- Matten LC, Banks HP. 1969.** *Stenokoleos bifidus* sp. n. in the Upper Devonian of New York State. *American Journal of Botany* **56**: 880-891.
- May BI, Matten LC. 1983.** A probable pteridosperm from the uppermost Devonian near Ballyheigue, Co. Kerry, Ireland. *Botanical Journal of the Linnean Society* **86**: 103-123.
- Momont N. 2015.** *Investigation of basal lignophytes: the Aneurophytales and the Stenokoleales re-examined*. Ph. D. thesis, University of Liège, Liège, Belgium.
- Momont N, Gerrienne P, Prestianni C. 2016.** *Brabantophyton*, a new genus with stenokolealean affinities from a middle to earliest Upper Devonian locality from Belgium. *Review of Paleobotany and Palinology* **227**: 77-96.
- Galtier J. 1988.** Morphology and phylogenetic relationships of early pteridosperms. In: Beck CB, ed. *Origin and evolution of gymnosperms*. New York, USA: Columbia University Press, 135-176
- Gerrienne P, Gensel PG, Strullu-Derrien C, Steemans HLP, Prestianni C. 2011.** A simple type of wood in two Early Devonian plants. *Science* **333**: 837.

- R Core Team. 2017.** R: a language and environment for statistical computing. v. 3.4.1. *R Foundation for Statistical Computing*. [WWW document] URL <https://r-project.org>. [accessed 11.01.2017].
- Read CB. 1938.** Some Psilophytales from the Hamilton Group in Western New York. *Bulletin of the Torrey Botanical Club* **65**: 599-606.
- Remy W, Hass H. 1986.** *Gothanophyton zimmermanii* nov. gen. nov. spec., eine Pflanze mit komplexem stellar Körper aus dem Emsian. *Argumenta Paleobotanica* **7**: 9-69.
- Rothwell GW. 1999.** Fossils and ferns in the resolution of land plant phylogeny. *Botanical Review* **65**: 188-218.
- Rothwell GW, Nixon KC. 2006.** How does the inclusion of fossil data change our conclusions about the phylogenetic history of euphyllophytes? *International Journal of Plant Sciences* **167**: 737-749.
- Scheckler SH. 1976.** Ontogeny of progymnosperms. I. Shoots of Upper Devonian Aneurophytales. *Canadian Journal of Botany* **54**: 202-219.
- Scheckler SH, Banks HP 1971.** *Proteokalon* a new genus of progymnosperms from the Devonian of New York State and its bearing on phylogenetic trends in the group. *American Journal of Botany* **58**: 874-884.
- Schweitzer HC, Matten JL. 1982.** *Aneurophyton germanicum* and *Protopteridium thomsonii* from the Middle Devonian of Germany. *Palaeontographica B* **184**: 65-106.
- Serbet R, Rothwell GW. 1992.** Characterizing the most primitive seed ferns. I. A reconstruction of *Elkinsia polymorpha*. *International Journal of Plant Sciences* **153**: 602-621.
- Serlin BS, Banks HP. 1978.** Morphology and anatomy of *Aneurophyton*, a progymnosperm from the Late Devonian of New York. *Palaeontographica Americana* **51**: 47-51.
- Spicer R, Groover A. 2010.** Evolution of development of vascular cambia and secondary growth. *New Phytologist* **186**: 577-592.
- Stein WE. 1982.** The Devonian plant *Reimannia* with a discussion of the class Progymnospermopsida. *Paleontology* **25**: 605-622.
- Strullu-Derrien C, Kenrick P, Tafforeau, Cochard H, Bonnemain JL, Le Herisse A, Lardeux H, Badel E. 2014.** The earliest wood and its hydraulic properties documented in

c. 407-million-year-old fossils using synchrotron microtomography. *Botanical Journal of the Linnean Society* **175**:423–437.

Toledo S, Bippus AC, Tomescu AMF. 2018. Buried deep beyond the veil of extinction: euphyllophyte relationships at the base of the spermatophyte clade. *American Journal of Botany* (in press).

Tomescu AMF. 2009. Megaphylls, microphylls and the evolution of leaf development. *Trends in Plant Science* **14**: 5-12.

Wilson JP 2016. Hydraulics of *Psilophyton* and evolutionary trends in plant water transport after terrestrialization. *Review of Palaeobotany and Palynology* **227**: 65-76.

Supporting Information

Figure S1. *Kenricrana bivena* gen. et sp. nov. main axis in Gaspé cobble and primary branch anatomy.

Figure S2. *Kenricrana bivena* gen. et sp. nov. anatomy of main axes.

Figure S3. *Kenricrana bivena* gen. et sp. nov. anatomy of main axes and ultimate appendages.

Figure S4. *Kenricrana bivena* gen. et sp. nov. structure of P-type secondary wall thickenings in metaxylem tracheids.

Figure S5. Strict consensus tree generated by analysis using discrete characters only.

Figure S6. Majority rule consensus tree generated using discrete characters only.

Figures

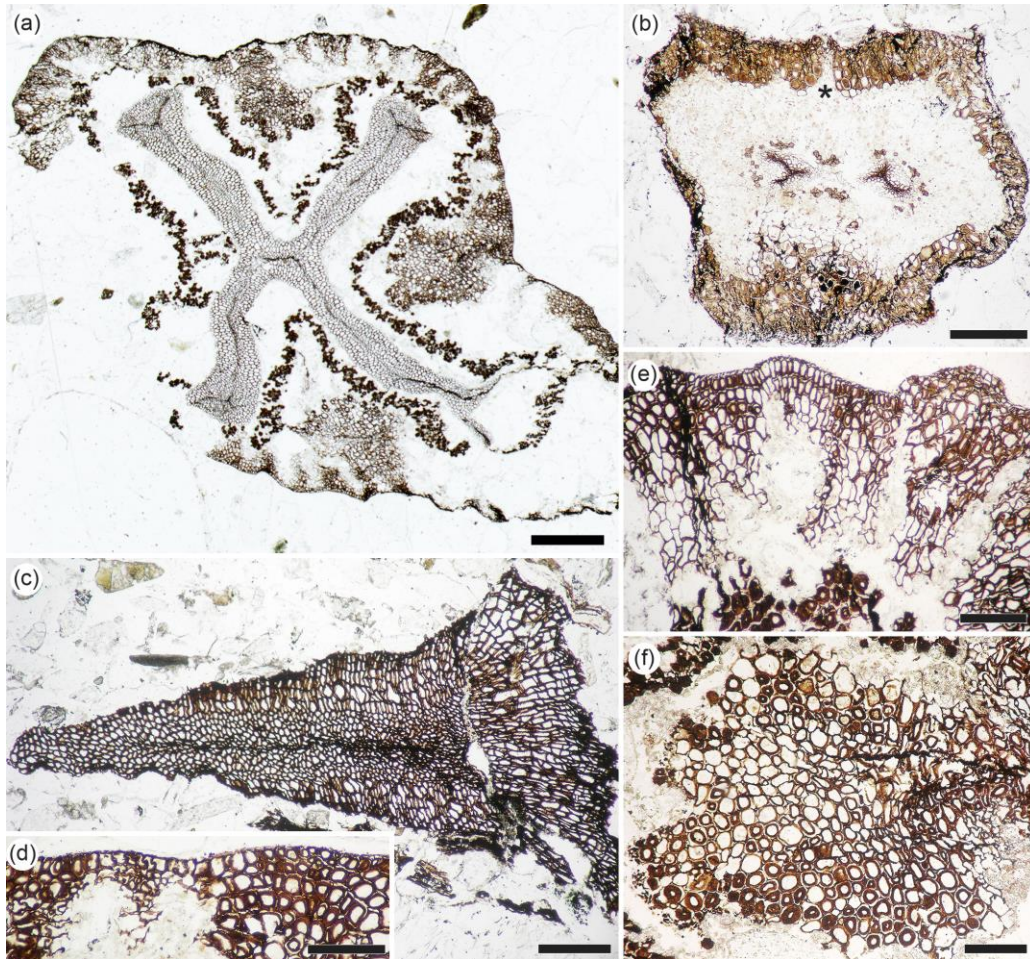


Figure 1 *Kenricrana bivena* gen. et sp. nov. anatomy. **(a)** Main axis cross section; note four-ribbed actinostele with protoxylem along rib midplanes and at rib tips; tangentially expanded rib tips and rib tip protoxylem, basal to divergence of traces to primary branches; discontinuous layer of sclerenchyma in inner cortex, following the outline of the xylem; outer cortex with *Sparganium* anatomy; large sclerenchyma clusters protruding from the outer cortex in the sectors corresponding to the areas between xylem ribs (top, bottom, and right); compare with Supporting Material Fig. S2; USNM 557820-5 #2a; bar 700 μm . **(b)** Primary branch cross section; note two Y-shaped xylem bundles; broad parenchymatous inner cortex with discontinuous layer of sclerenchyma close to and around xylem; primarily sclerenchymatous outer cortex interrupted by substomatal chamber (asterisk); compare with Supporting Material Fig. S1b,c; USNM 55783-1 Dtop #2a; bar 400 μm . **(c)** Fragmentary specimen consisting of primary xylem rib with secondary xylem around tip and sides; note protoxylem along rib midplane and radially aligned secondary xylem tracheids; USNM 557840 Jtop #5b; bar 400 μm . **(d)** Detail of (a); note epidermis and *Sparganium* outer cortex with alternating sectors of sclerenchyma and parenchyma (incompletely preserved); bar 200 μm . **(e)** Main axis cross section; epidermis, *Sparganium* outer cortex, and part of the discontinuous sclerenchyma layer of inner cortex (bottom); USNM 557820-5 #80a; bar 200 μm . **(f)** Detail of (a); large sclerenchyma cluster in sector between two xylem ribs; note irregular cell size and cell wall thickness; bar 200 μm .

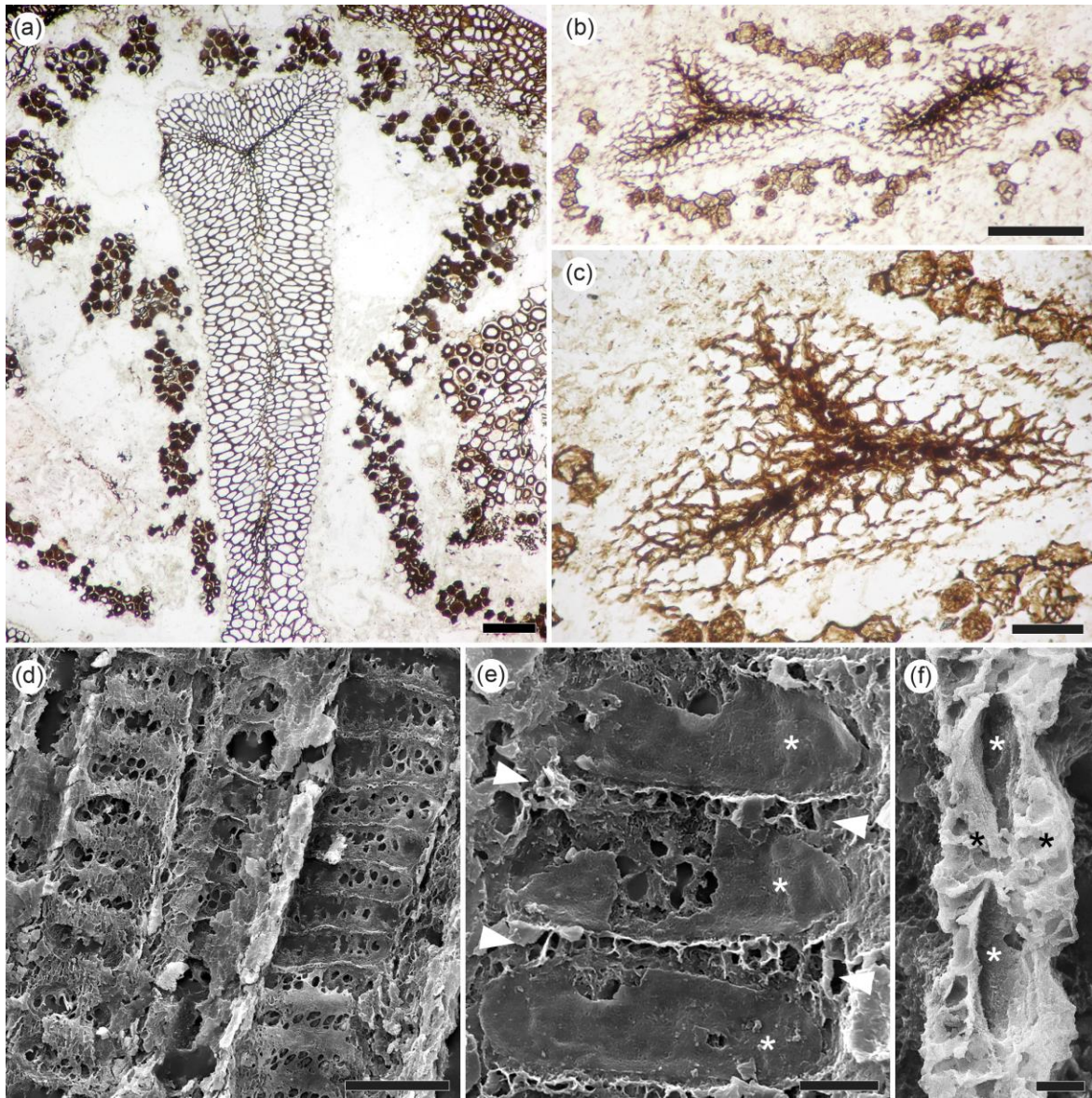


Figure 2 *Kenricrana bivena* gen. et sp. nov. anatomy. (a) Main axis cross section; primary xylem rib with protoxylem along midplane and at rib tip; note tangentially expanded rib tip and protoxylem, basal to divergence of trace to primary branch; nests of sclerenchyma forming discontinuous layer around xylem, in inner cortex; compare with Supporting Material Fig. S3f; USNM 557820-5 #80a; bar 300 μm . (b) Primary branch cross section; detail of vascular bundles, one Y-shaped, the other asymmetrical (due to divergence of ultimate appendage trace); note discontinuous layer of sclerenchyma around xylem; USNM 55783-1 Dtop #74b; bar 200 μm . (c) Detail of (b); note incompletely preserved phloem around xylem (arrowheads); bar 50 μm . (d) Metaxylem tracheids with P-type pitting; USNM 557839-4 Dtop #6 and 10; bar 25 μm . (e) P-type pitting of metaxylem seen in exposure created by detachment of two adjacent tracheids; pit membranes at asterisks; arrowheads indicate rupture areas produced by separation from adjacent tracheid (see Supporting information Fig. S4b for details); USNM 557839-4 Dtop #6 and 10; bar 5 μm . (f) Longitudinal section of two adjacent metaxylem tracheid walls forming pit pairs (pit chambers at white asterisks); note spongy structure of secondary wall thickenings (black asterisks) (see Fig. S4a for details); USNM 557839-4 Dtop #6 and 10; bar 2.5 μm .

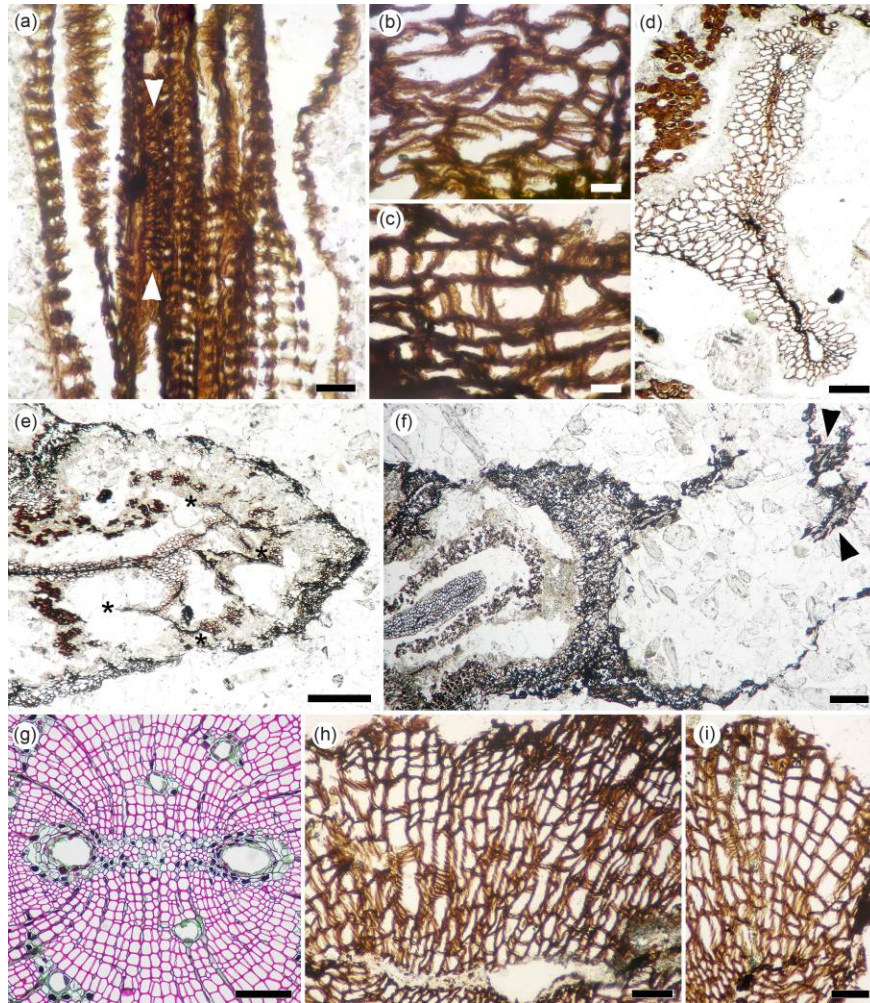


Figure 3 *Kenricrana bivena* gen. et sp. nov. anatomy. (a) Main axis primary xylem longitudinal section; note metaxylem with P-type pitting and protoxylem with annular-helical thickenings (between arrowheads); USNM 557839-4 Dtop #20a; bar 25 μ m. (b,c) Secondary xylem cross section showing P-type pitting on radial (b) and tangential (c) tracheid walls; USNM 557840 Jtop #5b; bars 25 μ m. (d) Main axis cross section; divergence of trace to primary branch; tip of primary xylem rib tangentially expanded preceding (basal to) trace divergence; note protoxylem gaps at both tips of T-shaped rib tip; USNM 557839-2b Atop #68c; bar 150 μ m. (e) Main axis cross section; divergence of trace to primary branch; tip of primary xylem rib tangentially expanded in T shape; tips of the T-bar also laterally expanded (asterisks); note discontinuous layer of sclerenchyma nests that follows outline of the expanded primary xylem rib tip; USNM 557839-2b Atop #1c; bar 600 μ m. (f) Main axis cross section; divergence of trace to primary branch (at right) consisting of two Y-shaped vascular bundles (arrowheads); note round shape of primary xylem rib tip distal to trace divergence (at left); USNM 557839-1 Atop #1a; bar 500 μ m. (g) *Pinus* root cross section exemplifying anatomy of wood produced in early stages of secondary growth in a protostelic axis; note scarcity of multiplicative divisions in the portion produced by first 10-12 cambial divisions and often inconspicuous rays in the same tissue; compare with *Kenricrana* secondary xylem in Fig. 3h,i; bar 200 μ m. (h,i) Secondary xylem of *Kenricrana*; the conspicuous increase in number of tracheid files from bottom (adjacent to primary xylem) toward the top (periphery of secondary xylem) is consistent with multiplicative divisions; USNM 557840 Jtop #5d and Ibot #1b, respectively; bars 100

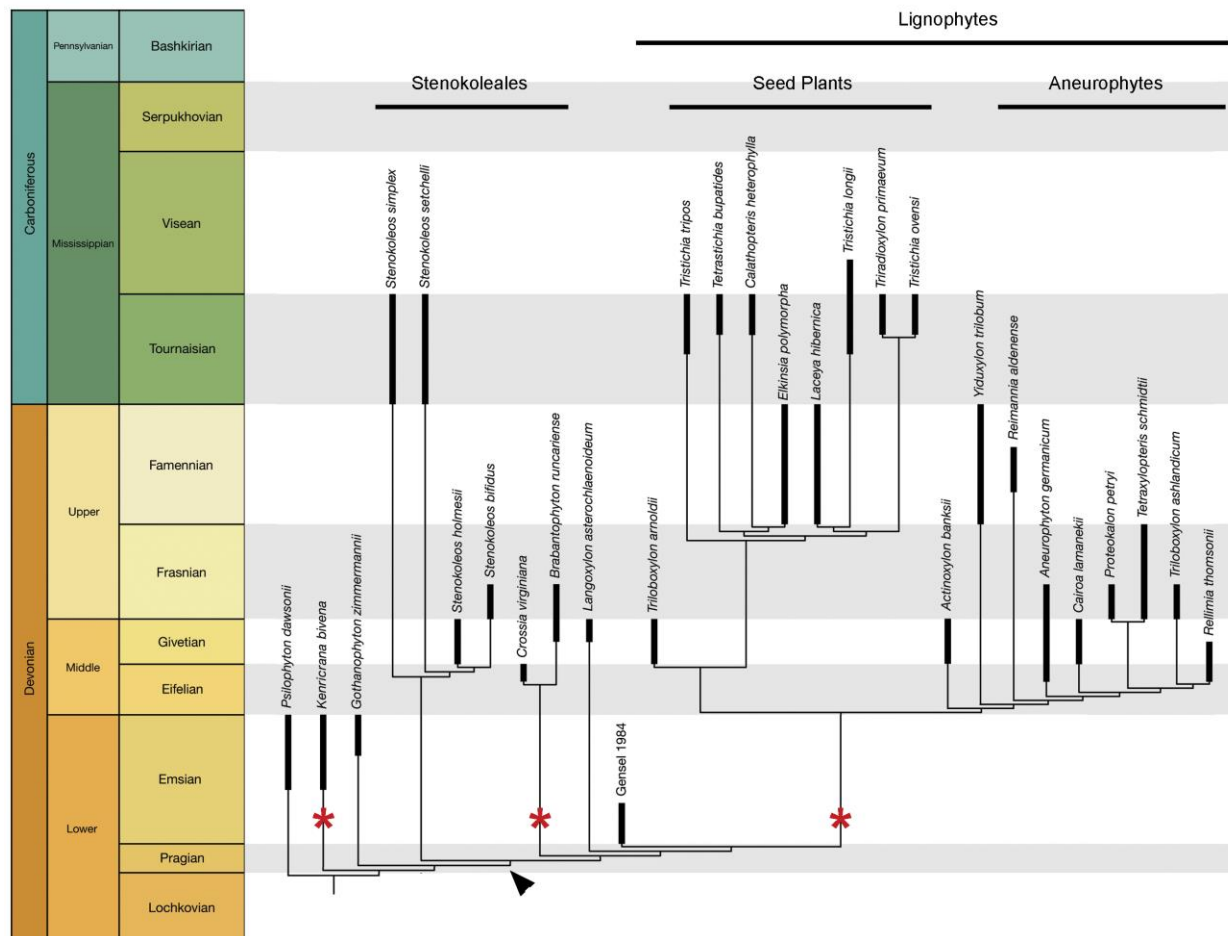


Figure 4 Time-calibrated maximum parsimony tree (tree length 102.78; CI = 0.49, RI = 0.60) generated using discrete and continuous characters, and constrained by fossil ages. *Kenricrana* is sister to the rest of the ingroup; along with two stenokolealean clades, *Gothanophyton*, *Langoxylon*, and Gensel's (1984) plant, *Kenricrana* is part of a paraphyletic grade that leads up to the lignophyte clade including seed plants and aneurophytes; arrowhead – adaxial-abaxial polarity, as reflected in xylem anatomy (lost in aneurophytes and Gensel's plant); asterisks – lineages exhibiting secondary growth.

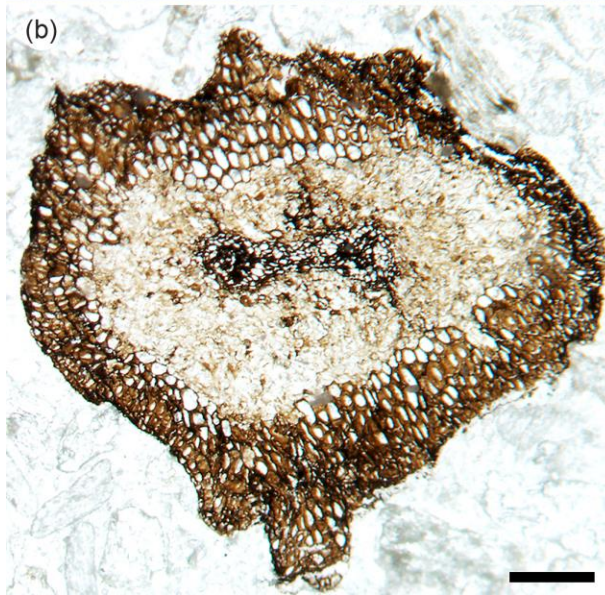
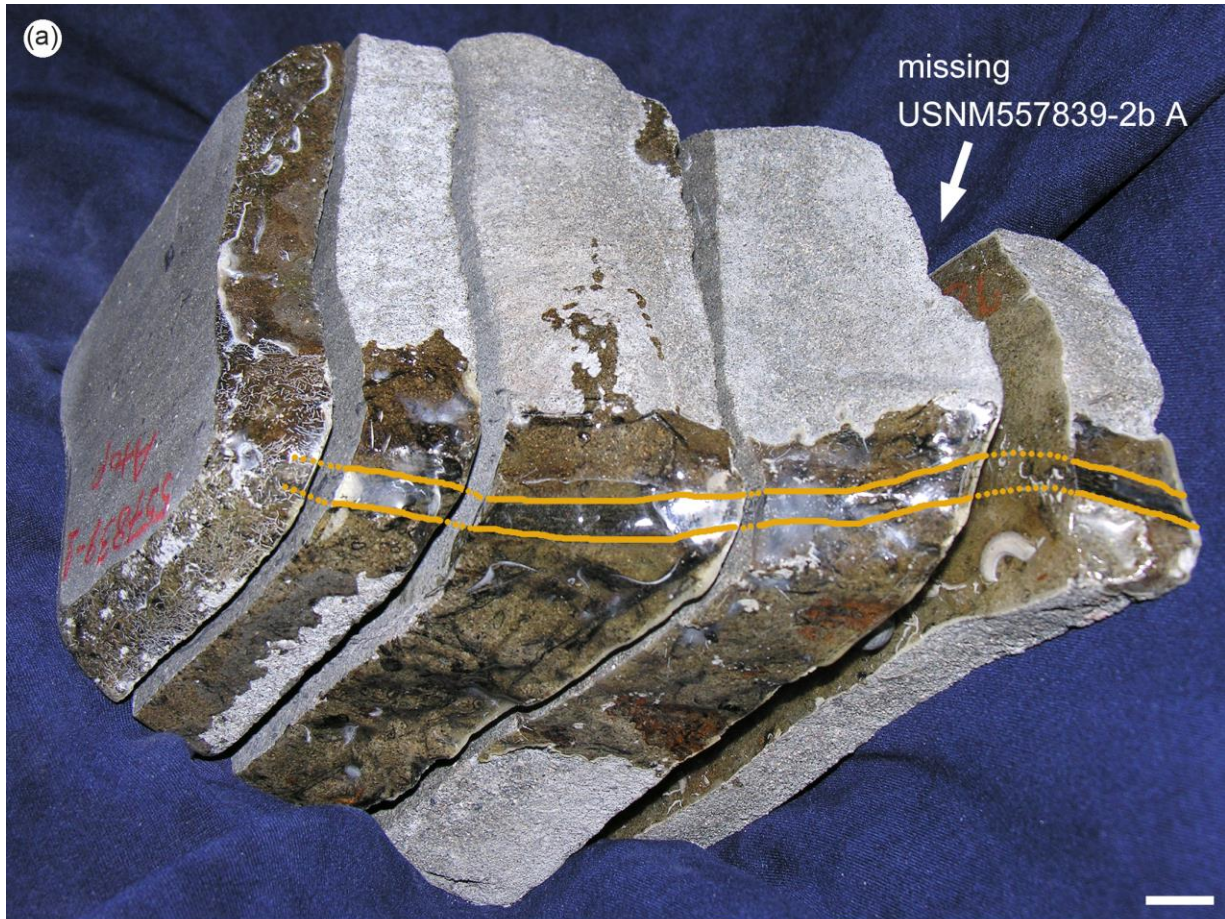


Figure S1. *Kenricrana bivena* gen. et sp. nov. main axis in Gaspé cobble and primary branch anatomy.

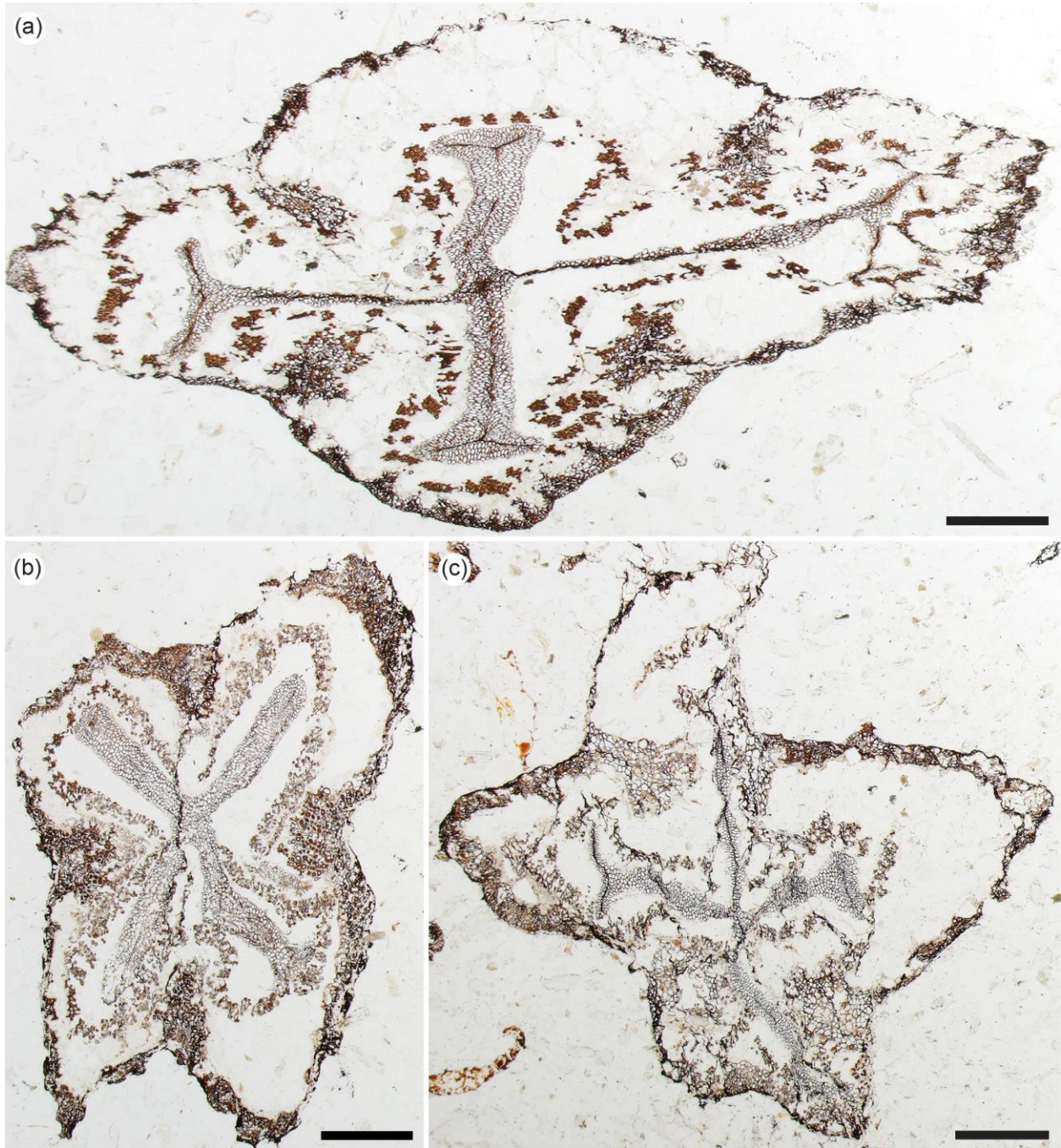


Figure S2 *Kenricrana bivena* gen. et sp. nov. anatomy of main axes.

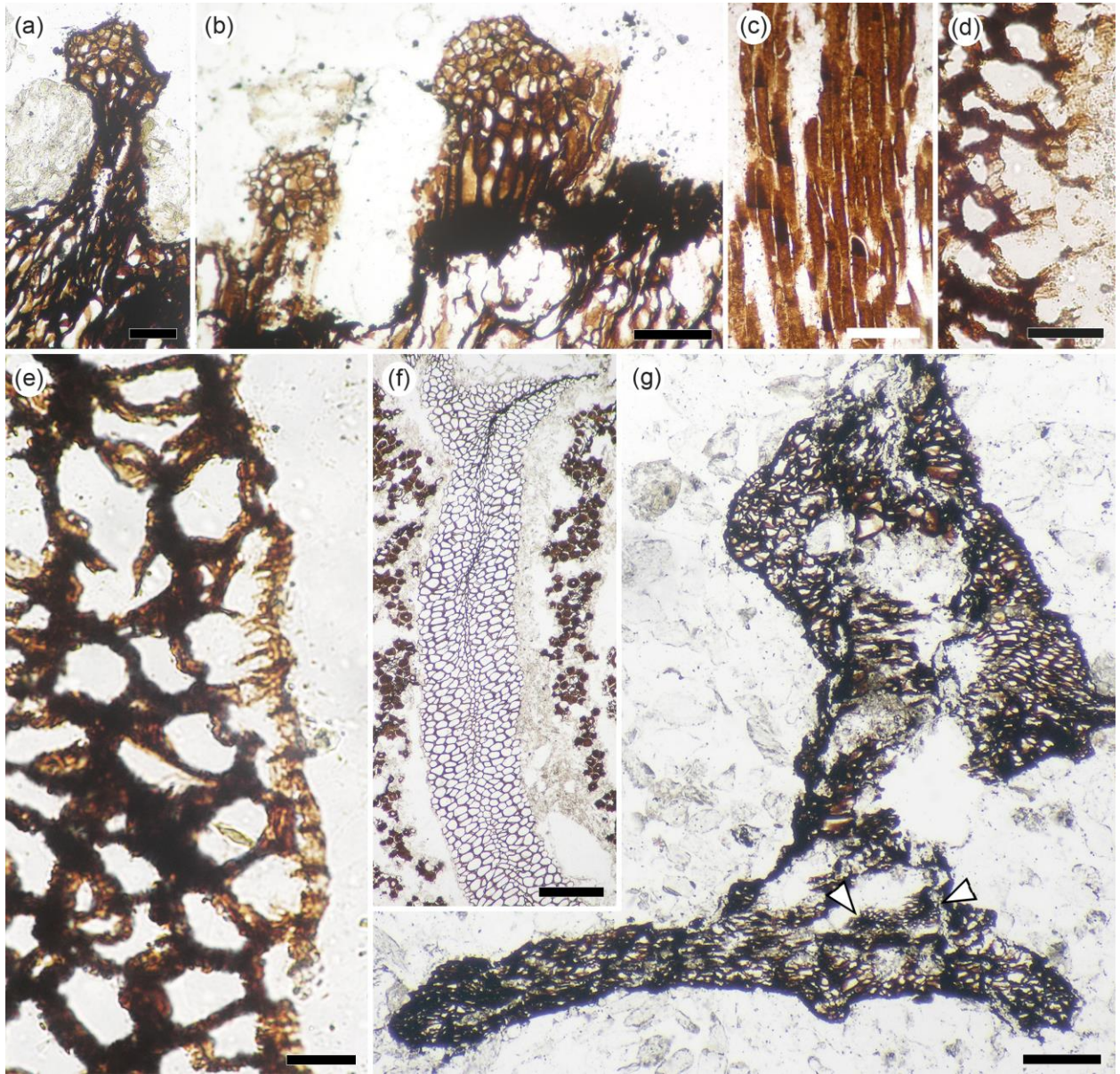


Figure S3 *Kenricrana bivena* gen. et sp. nov. anatomy of main axes and ultimate appendages.

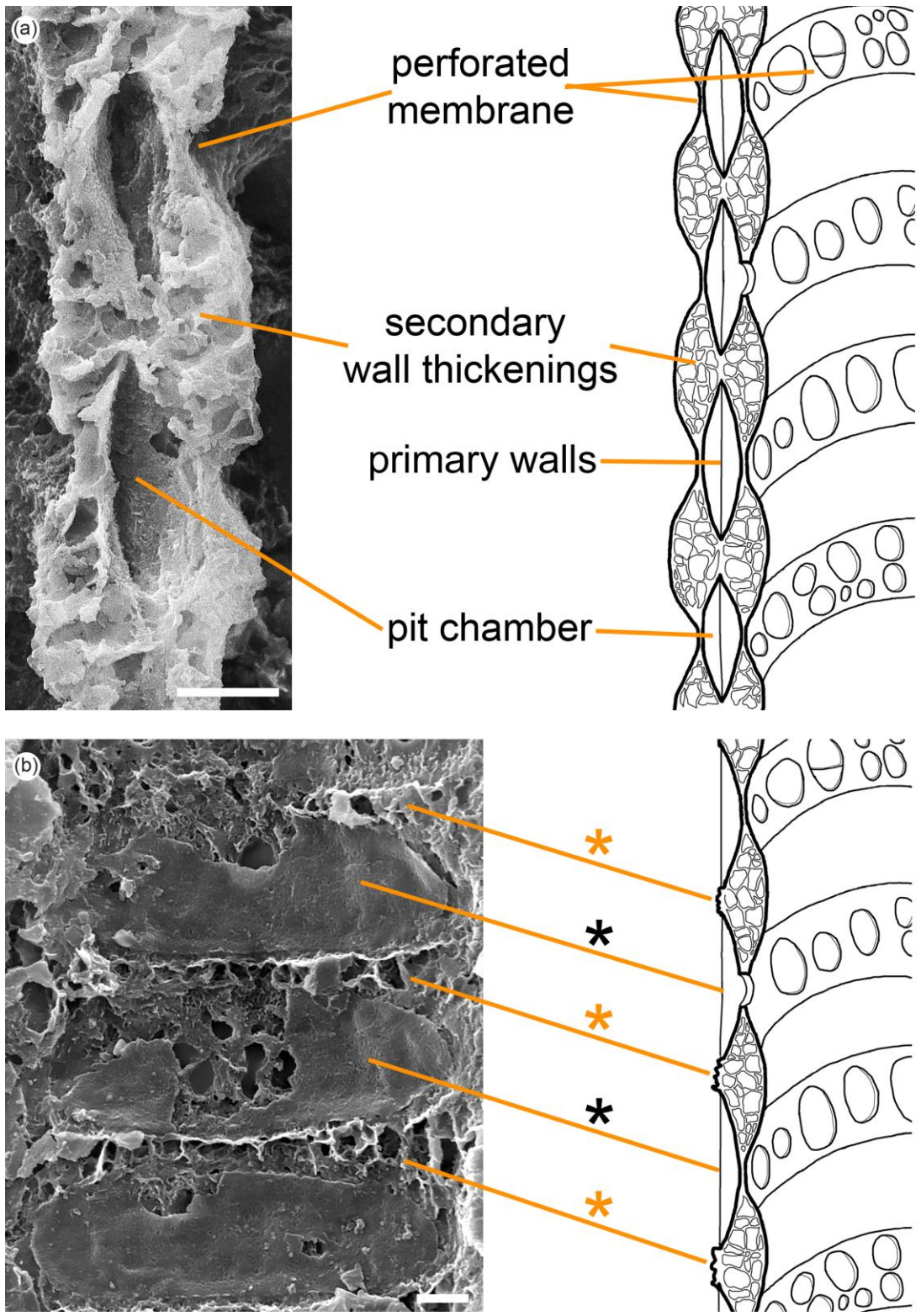


Figure S4 *Kenricrana bivena* gen. et sp. nov. structure of P-type secondary wall thickenings in metaxylem tracheids.

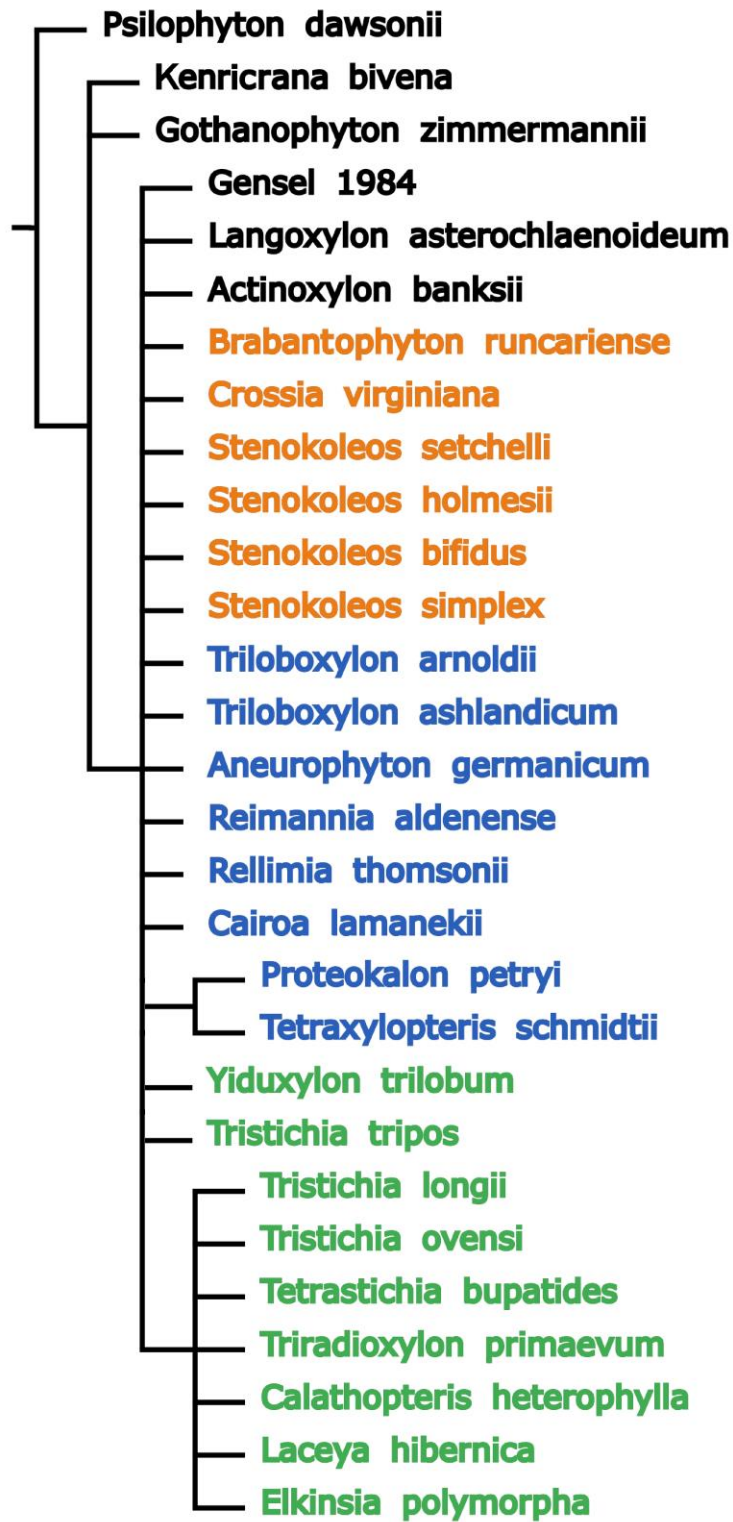


Figure S5 Strict consensus tree generated by analysis using discrete characters only.

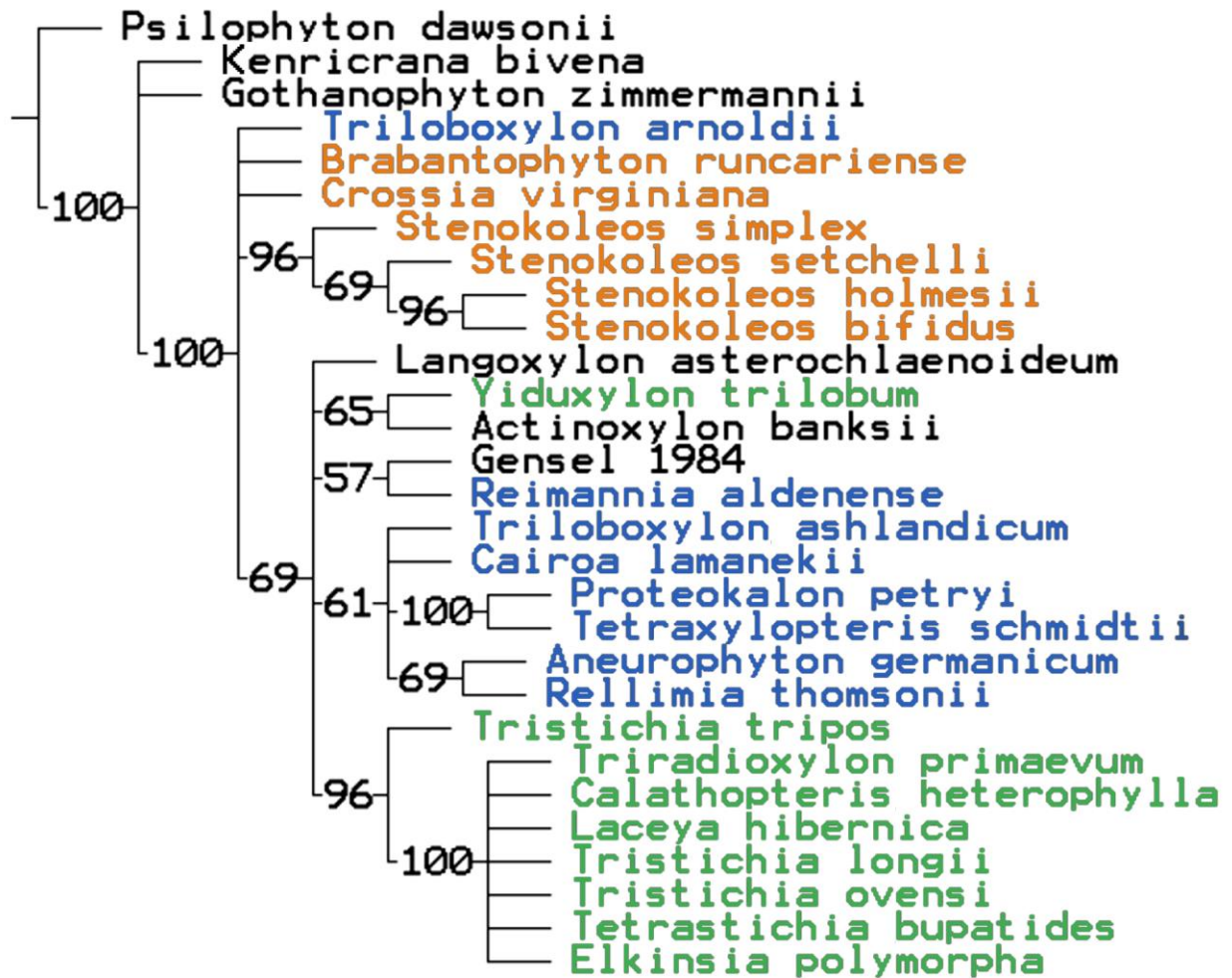


Figure S6 Majority rule consensus tree generated using discrete characters only.